Study for the effect of pressure, size and shape of nanomaterials

Thesis

Submitted to the

G. B. Pant University of Agriculture & Technology
Pantnagar- 263145, Uttarakhand, India

By

Laxmi Mehra
Id.No. 53943

IN PARTIAL FULFILMENT OF THE REQUIREMENTS FOR THE DEGREE OF

Master of Science
(Physics)

December, 2020

ACKNOWLEDGEMENT

Pride, praise and perfection belong to Almighty alone. So, first of all, I would like to thank 'HIM' for health and courage he bestowed on me to go through this crucial juncture.

I bow before my parents in utter reverence. No words can suffice my feelings of monumental gratitude for the moral support, encouragement, affection, patience and ever willing help rendered by my family. I owe a lot to my father Khushal Singh, my mother Mrs. Jasoda, my elder sister Swati Rawat and my brother Dhiraj Singh for his benediction, love and sacrifice, who have always stood by me throughout my life.

Words in my lexicon, fails to elucidate my profound sense of veneration and indebtedness to Dr. Munish Kumar, Professor, Department of Physics and Chairman, Advisory Committee for his meticulous guidance, outstanding co-operation, encouragement, calm endurance and diligence, helped me to accomplish this work. I simply felt myself blessed being provided with an academic advisor like him. His keen interest towards science, scientific attitude, endless patience, and untiring cooperation helped me not only during the course of investigation and preparation of this manuscript but also at every step of my life in Pantnagar.

I considered it my privilege to thank all the esteemed members of my Advisory Committee, Dr. S.B Singh, Professor Department of Mathematics, Statistics and Computer Sciences and Dr. Puja Goel, Assistant Professor, Department of Physics for their valuable suggestions and fruitful blessings.

I wish to extend my sincere thanks to Librarian, Director, Dean, College of Post Graduate Studies and Registrar for providing me the essential facilities to me during my studies. I also express my gratitude to all faculty members as well as academic and non-academic staff, Department of Physics for their help and cooperation.

The pleasant company, co-operation and help melted out by my respected senior who always guided me for betterment of my work. There are no words to pay my regards to Soni mam for being my guide during the period of my study and for their constant support, help and goodwill for me.

I am thankful to my batchmates who helped me a lot and provided me full time support, Nidhi, Neha, Deepti, Rashmi, Kamal, Rajat, Deepak, Raj, Tikendra and Manish. Also I would like to thank my juniors for their constant support.

Lastly, special thanks to all my loved ones, Munmun, Gayatri, Anjali, Sudarshana, Pranjal, Pawan, Manisha, Himani, Dharma, Deepak and Chandan for always motivating and supporting me directly and indirectly throughout my entire degree programme.

Finally the financial assistance rendered by the university is duly acknowledged.

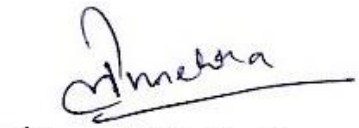

Pantnagar
December, 2020

(Laxmi Mehra)
Authoress

CERTIFICATE

This is to certify that the thesis entitled **"Study for the effect of pressure, size and shape of nanomaterials"** submitted in partial fulfilment of the requirements for the degree of **Master of Science** with major in **Physics** from College of Basic Sciences and Humanities, G.B. Pant University of Agriculture and Technology, Pantnagar, is a record of bonafide research carried out by **Ms. Laxmi Mehra, Id. No. 53943,** under my supervision, and no part of the thesis has been submitted for any other degree or diploma.

The assistance and help received during the course of investigation and source of literature have been duly acknowledged.

(Munish Kumar)
Chairman
Advisory committee

Pantnagar
December, 2020

CERTIFICATE

We, the undersigned members of Advisory Committee of **Ms. Laxmi Mehra,** Id. No. **53943,** a candidate for the degree of **Master of Science** with major in **Physics** agree that the thesis entitled **"Study for the effect of pressure, size and shape of nanomaterials",** may be submitted in partial fulfillment of the requirements for the degree.

(Munish Kumar)
Chairman
Advisory Committee

(S.B. Singh)
Member

(Puja Goel)
Member

CONTENTS

LIST OF TABLES

LIST OF FIGURES

Introduction

On 29 Dec 1959, Nobel laureate and physicist **Richard P. Feynman** gave a historical talk at the American Physical society that provoked many to think small down to the order of atoms and molecules and marked the onset of a new technology called as "nanotechnology", he presented a classic lecture on the topic **"There's Plenty of Room at the Bottom"**. The term "Nanotechnology" was first introduced by **Taniguchi** in 1974 in a paper entitled **"On the Basic Concepts of Nanotechnology",** he stated that nanotechnology mainly consists of the processing of separation, consolidation and deformation of materials by one atom or one molecule.

The word 'nano' comes from the Greek word 'nanos' or latin word 'nanus' that means 'Dwarf'. Nanomaterials are defined as the materials where the sizes of the individual building blocks are less than 100nm at least in one dimension or the nanomaterials have properties that depend inherently on the small grain size. As moving from bulk to the nanoscale may lead severe changes in the chemical and physical properties of material. Nanoscience is the study of materials between the size range (1-100nm). Nanomaterials may be zero-dimensional (nanoparticles), one-dimensional (nanorods or nanotubes), or two-dimensional (usually realized as thin films or stacks of thin films). Quantum confinement effects or the increasing prevalence of surface atoms drives physical evolutions between bulk and nanoscaled materials.

Nanomaterials shows novel properties which has led to an extensive interest into them. Nanoparticles are used in a variety of application, such as sensors, LEDs, drug delivery, medical diagnostics, catalyst and gene therapy. Their unique range of properties and enormous application led to the development of the nanotechnology.

As the materials are reduced to nanoscale they show very different properties compared to bulk, because of this nanomaterials received more attention due to their unique physical, chemical, mechanical, optical, thermal, electrical and magnetic properties, in comparison to their bulk counterpart. The material properties of nanostructures are different from the bulk basically due to high surface to volume ratio and quantum

confinement effect. Due to their small dimensions, nanomaterials have extremely large surface area than bulk materials. Suppose we have a sphere of a radius, then surface to volume ratio is 3/a. It means the ratio is inversely proportional to the radius. If the radius of sphere reduces then surface to volume ratio increases and vice-versa. When the sizes of nanomaterials are comparable to length, the entire material is affected by surface dependent material properties. For example, metallic nanoparticles are used as very active catalysts. The nanomaterials also have spatial confinement effect on materials which bring the quantum effects. The quantum confinement effect is observed when the size of material is too small comparable to the wavelength of electron. In nanocrystal, the electronic energy levels are discrete (finite density of states), because of the confinement of the electronic wave function to the physical dimensions of the particles. This phenomena is quantum confinement and the nanocrystals are known as quantum dots. Because of their unique properties, quantum dots have many applications in different fields including solar cells, LEDs, Transistors, displays, laser diodes, medical imaging etc.

NSMs can be classified into following categories:

1. Zero-Dimension (0-D): all dimension in nanoscale range. Examples are QDs.
2. One-Dimension (1-D): Two dimension in a nanometre range, less than 100nm are typically nanofibers, nanowires, nanorods and nanotubes.
3. Two-Dimension (2-D): having one dimensions in nanometer range and it includes nanofilms, monolayer, multilayer, self-assembled, and plates etc.
4. Three-Dimension (3-D): no dimension in nanoscale range and it includes nanocomposites, nanohybrids, micro and mesoporous hybrid, nanometer-sized grains.

Due to the large surface to volume ratio of nanomaterials the surface atoms play an important role to demonstrate the thermodynamic properties. Generally Equaton of state is a relationship between state variables like pressure temperature and volume but this definition is not applicable for nanomaterials because of the size factor between bulk and nanomaterials so in case of nanomaterials the definition is a relationship between the state

variables like pressure, volume, temperature and size. As size is an important factor in this so we have to study about size dependence of EOS to understand the behaviour of nanomaterials under high pressure. Size dependency is further more complicated when surface factor are responsible for unique properties of the nanomaterials.

The EOS is a thermodynamical relation which explains the dependence of one parameter on other parameters. An EOS can be applied successfully to explain the behaviour of solids under varying pressure and temperature. The universal form of EOS for pressure as well as a function of volume for different classes of solids in compression was discovered by **(Vinet *et al.,* 1986)**. Several theoretical and experimental studies have been performed during past to explain the behaviour of solids under varying temperature pressure conditions and a well-known EOS for solids is given by Murnaghan **(Murnaghan, 1937).**

The physical properties of materials depend strongly on the structure and interatomic distances, high pressure and high temperature can vary these distances. On varying temperature and pressure on nanomaterials many transformation effects occur. As bulk modulus measures the compressibility so it is evident that change in particle size affect the bulk modulus of material directly. The value of bulk modulus increases with decrease in the size. The change in size from bulk to nano leads to change in surface energy and reduction in volume which results in extra binding energy in nanomaterials as compared to their bulk counterparts. The increase in surface energy tends to increase in bulk modulus viz. reduction of compressibility in nanomaterials.

Size plays an important role in nanomaterials, there have been a number of studies on the size dependent behavior of thermal properties for nanomaterials **(Qi *et al.,* 2003; Qu *et al.,* 2017)**. CE is another important factor which define the strength of metallic bond. **Nanda et al. (2002)** used the liquid drop model for the size dependence of CE of nanosolid. **Qi and Wang (2002)** they developed a simple method to calculate the CE of nanoparticles and this method showed that the CE depends on particle size i.e the CE increases with a increase in particle size and vice versa. **Qi and Wang (2004)** proposed a new model on account for the effect of shape and size on the metallic nanoparticles. They considered a particle shape difference by introducing a shape

factor. They showed that the particle shape affects the melting temperature of nanoparticles and particle shape factor increases with decreasing the particle size.

The thermodynamic properties under high pressure are very important and many experimental and theoretical models were proposed. **Bhatt *et al.* (2013)** made an effort to find a suitable EOS for nanomaterials. They used six different models to study the compression behaviour of nanomaterials and got the best result for murnaghan EOS for thirty one naomaterials. **Kumar and Kumar (2013)** discussed a simple thermodynamical EOS and used to study the isothermal compression behaviour and pressure dependence of bulk modulus for nanomaterials. **Qi (2016)** studied the nanoscopic thermodynamics and highlighted some points for nanoparticles, nanowires and nanofilms using BEM. His main focus is on the CE which determines the thermodynamic performance of material and CE depend on the coordination environment. The BEM is used to rationalize the effect of surface dangling bonds which depress the melting temperature, entropy, enthalpy, Gibbs free energy and formation heat, defined the dependence on nanoparticles size how their stability vary when they are embedded in an appropriate matrix. The model was also useful to study the superheating phenomenon, thermal stability of metal particles on graphene, order-disorder transition of nano alloys, and size-temperature phase diagram for nanoparticles. **Kumar and Bhatt (2017)** developed a model to study the effect of size, shape, temperature and pressure, used to study the EOS and pressure dependence on SnO_2 nanomaterial. The model is also used to study the compression behaviour at room tempertature and they compared the results with experimental data as well as with Birch-Murnaghan equation of state**. Chhabra and Kumar (2020)** developed a simple model based on the bond energy analysis and used to compute the size and shape dependence of magnetic properties. They found that T_c (D) and Ms(D) decreases with decrease in size and T_N(D) increases or decreases with drooping D.

As nanomaterials having a great potential to provide social benefit so nanostructured materials are the focus point for all the researchers. Mainly the properties of nanomaterials depends on pressure, size and shape. There have been a numbr of experimental and theoretical models to study the effect of size, shape, temperature and pressure. In the present work we study for the effect of pressure, size and shape of nanomaterials. The main objectives of our planned work are as follows.

- In the present work, we shall modify the Murnaghan EOS to study the behavior of nanomaterial under the effect of pressure for nanomaterials of current interest.
- The model thus formulated shall be used to study the compression behavior of nanomaterials.
- The model shell be used to study the compression behavior of different nanomaterials for size.
- Further we shall extend the model to study the shape effect on nanomaterials.
- We shall compare our results with the available experimental data to demonstrate the suitability of the formulation used in the present work.

The thesis is divided into five different chapters. Chapter 1 provides a brief introduction. Chapter 2 is a review of literature. Chapter 3 is about the material and methods. Chapter 4 the results are discussed. Chapter 5 gives the overall summary of the present work. Literature cited are given in last.

Review of Literature

Several experimental, theoretical models have been proposed to study the thermodynamical behavior of nanoparticles under the effect of size, shape, temperature and pressure. The study with varying thermodynamical parameters can help us to find useful materials, the present chapter is all about the literature review of the same work.

Murnaghan (1937) showed, how the observed effect of the change of compressibility with pressure is readily accounted in terms of his theory of finite strain. He was the first who proposed equation of state (EOS). **Vinet *et al.* (1986)** discovered a universal EOS for solids, there is a universal form for pressure as a function of volume for all the classes of solids in compression. **Plymate *et al*. (1989)** derived an explicit empirical V(T,P) equation based on an exponential temperature correction of the Isothermal Murnaghan equation. They successfully tested equation against literature pressure -volume-temperature (P-V-T) data for NaCl. **Anderson (1995)** gave equation of states of solids for geophysics and ceramic science. Developed a theory showing how the thermoelastic parameters vary with *T* and *V* at high temperature and high compression. Also emphasized α and its relationship to many properties in the EOS and cast it in terms of thermoelastic dimensionless parameters. The varation of α with *T, V,* and *P* at extreme conditions is presented. **Kumar (1995)** reported a simple equation of state to investigate the properties of solids under high pressures. He studied the compression behavior for sodium halides, viz. NaF, NaCl, NaBr and NaI from atmospheric pressure to their transition pressures. The results were found with the better agreement with the Murnaghan EOS, which is applicable only upto 40 Kbar (low pressure range) but the equation proposed by this paper is applicable upto transition temperature.

Jiang *et al.* (1997) developed a model for the dependence of melting temperature of nanocrystals on the size of carbon nanotube. They have considered the nanotube size dependent melting of TaC and Pb single crystals in carbon nanotubes, and the results were found that the melting temperature for these crystals can be strongly suppressed and depicted that the carbon nanotubes as an effective way to

investigate the supercooled state of liquids and liquid-glass transition. **Hama *et al.* (1999**) proposed a simple method to calculate the thermoelastic properties of MgO under high pressure and high temperature. The model was successful to explain the thermoelastic properties of MgO with experimental EOS at room temperature of 220Gpa pressure and EOS of shock-wave 200Gpa. The input parameters used here are the volume of unit cell, bulk modulus, pressure derivative of bulk modulus and Debye temperature at room temperature and zero pressure. The author also discussed about the thermal expansivity, experimental velocities compressional and shear waves with a wide temperature and zero pressure. They also calculated the thermal EOS and shock wave EOS. **Shanker *et al.* (1999)** developed a new criterion for melting on the basis of the thermal equation of state based on the method of lattice potential energy. The results obtained for the melting temperature and its pressure dependence are presented in case of NaCl, KCl, MgO and CaO. **Jiang *et al*. (1999)** proposed a theoretical model for the size dependent melting temperature and the size dependent melting entropy. organic nanocrystals exhibit less melting temperature and melting entropy because the vibrational spectrum of the surface region is different for bulk. With decreasing crystal size all these effects increases.

Zhang (2000) reported an isobaric thermal expansion data of MgO at pressures of 2.6, 5.4, and 8.2 GPa in the temperature range 300 to 1073 K. The experiments were performed using DIA type, large-volume apparatus designed for in-situ X-ray diffraction studies at simultaneously high pressure and temperature. **Rekhi *et al*. (2000)** performed an X-ray diffractrometry to investigate the effect of particle size on compressibility of MgO (1000 and 2000Å). They found that the bulk modulus of MgO is independent with particle size. **Qadri *et al*. (2001)** studied the pressure induced phase transformations for the two different sizes of ZnS nanoparticles (2.8 and 25.3nm) using X-ray diffraction and diamond anvil cell. They found that the the zinc-blende particles (2.8nm) and wurtzite particles (25.3nm) particle size transformed into NaCl phase at 19 and 15GPa pressure respectively. They also found that the nanoparticles of the wurtzite never returned to their initial structure but the Zinc blende phase returned to their original on release of pressure. **Qi *et al*. (2002)** developed a simple method to calculate the cohesive energy of nanoparticles, as the cohesive energy is the heat of sublimation. They observed that the cohesive energy of nanoparticles depend on its

size, with increase in size the cohesive energy is also increased and when the particle size is large enough the cohesive energy will approach its bulk value.

Chen *et al*. (2002) showed that the compressibility increases with decreasing size for nanocrystalline γ-alumina by high pressure quasihydrostatic X-ray diffraction method. A new phase transformation has been observed by them. **Jiang *et al*. (2002)** proposed a model for the size dependence of latent heat and CE. They found that the CE decreases with decreasing particle size, the results were matched with the experimental data of CE for Mo and W nanoparticle. **Nanda *et al*. (2002)** established empirical relationship between the CE, surface tension, and melting temperature for different bulk solids. An expression was derived for the size dependent melting temperature on the low dimensional system by help of liquid drop model. The model was extended to understand the superheating of nanoparticles embedded in a matrix and the effect of size deposited cluster on a substrate temperature. When a nanoparticle with lower surface energy is embedded in a matrix with material of higher surface energy results superheating. **Olsen *et al.* (2002)** studied nc-TiO_2 by X-ray diffraction method at room temperature. They found a phase transformation to occur in the pressure range 20-30 Gpa from tetragonal to monoclinic. **Lu and Jiang (2004)** proposed simple model for size-dependent surface energy of nanocrystals, based on the earlier models proposed for the size dependent cohesive energy. The surface energy decreases with the decrease in nanocrystal size while the surface energy ratio between different facets is size independent and equal to the corresponding bulk ratio. The surface energies for Be, Mg, Na, Al and Au has been found from this model.

Qi and Wang (2004) proposed a new model for studying the dependency of particle shape and size on the melting temperature of metallic nanoparticles. The results obtained by reducing the size of nanoparticles and the particle shape effect on the melting temperature becomes larger. **He *et al.* (2005)** Studied high pressure behaviour of SnO_2 samples for bulk and nanocrystalline material by High pressure synchrotron radiation x-ray diffraction method. It was found that the smaller the SnO_2 nanocrystal higher the onset pressure for the phase transition from from rutile to cubic phase for nc-SnO_2, the increment in pressure is due to the surface energy differences between the phases. **Qi *et al*. (2005)** calculated the melting temperature for Sn and Pb nanoparticles

,nanowires, nanofilms by considering the surface effects based on size-dependent cohesive energy. The results showed that the melting temperature of free standing nanosolids decreased with the decrease in size. **Liang *et al.* (2005)** studied a molecular statics which is based on embedded-atom-method to find the elasticity of copper nanowires along crystallographic directions. It was found that on an comparison with bulk clearly showed that the overall nanowire elasticity is primarily due to nonlinear response of the nanowire core.

Liang and Baowen (2006) proposed a simple unified model for the size dependent elastic modulus and vibration frequency of nanocrystalline metals, ceramics and semiconductors based on the inherent lattice strain and the binding energy change of nanocrystals compared with the bulk counterpart, and the various nanomaterials are Cu, Ag, Si thin films and TiO_2 nanoparticles. **San-Miguel (2006)** reviewed the advantages and expected results with a effect of high pressure on nanomaterials. He demonstrated that the high pressure and high temperature are the effective tool for the modification of nanostructured materials. **Gilbert *et al*. (2006)** synthesized ZnS nanoparticles of different sizes to know the factors that determines compressibility of nanoparticles. They studied the high pressure X-ray diffraction to find out the compressibility of ZnS nanoparticles. They showed that the compressibility of ZnS nanoparticles increases with decreasing particle size. They studied both the bulk and nanoparticles and compared the results. **Pan *et al*. (2009)** synthesized ZnS nanoparticles for the average sizes 10nm and 5nm by sol-gel method. The pressure induced phase transition were examined by energy dispersive X-ray diffraction method. **Qi (2006)** generalized the surface area difference model (SAD) for the cohesive energy of nanoparticles with different composition in different shapes. It is found that the cohesive energy of nanoparticles with different composition depends on the nanoparticle size, the particle shape and the atomic percent of each composition. **Kumar and Kumar (2008)** studied EOS and the bulk modulus of nanosolids. The results obtained were in a good agreement with an experimental studies. **Luo *et al*. (2008)** obtained a method to calculate the thermodynamic properties of nanomaterials. Melting temperature, enthalpy of fusion, reduced heat capacity and entropy for Ag nanoparticles was found to be inversely to the reciprocal of particle size.

Chen *et al*. (2009) synthesized ZnO2 nanoparticles with an average particle size of 3.1nm by chemical method. They investigated Structural stability, magnetic and optical properties of nc-ZnO_2 by experiments and first-principles calculations. It was found that nc-ZnO_2 decompose into ZnO at about 230℃ and is stable up to 36 GPa at room temperature. nc-ZnO2 material is an indirect semiconductor with an energy gap of about 4.5eV and paramagnetic down to 5 K. **Lin *et al.* (2009)** investigated phase stability and compressibility of nanocrystalline tungsten carbide upto 35.6 GPa using synchrotron X- ray diffraction in a diamond anvil cell. It was found that the bulk modulus of nano WC is comparable to the diamond. **Couvy *et al*. (2009*)*** established an EOS for nc-FO (forsterite) using diamond anvil cell. They performed high temperature and high pressure experiments and found that nc-FO is more compressible than macro-FO. **Rich *et al*. (2009)** investigated high pressure X-ray diffraction for three different sizes of SiC (20, 50 and 130nm). The mulk modulus of the two larger sizes was consistent with bulk material whle the bulk modulus for the smaller one i.e 20nm was greatly increases. This observation was found to be consistent with the core-shell model which stated that the grain having size 20nm or smaller size possess compressed shell atoms. Moreover, on observing the results for the size 30nm the bulk modulus is smaller than the bulk modulus of size 20nm but larger than the 50nm grains. **Yao *et al*. (2009**) prepared ZnSe nanoparticles and studied both ZnSe nanoribbons as well as bulk ZnSe and compared both of them. High pressure ADXD was used to analyzed the structural stability of ZnSe nanoribbons, the phase transition occurs at 12.6 GPa from the Zinc blende to rocksalt. In their they observed that the effect of pressure on the change in volume suddenly becomes discontinuousat pressure 5.2 GPa, which shows the unidentified transition. **Kumar *et al.* (2010)** proposed a model to study the thermal expression and compression of nanoparticles, which demonstrates that the two different approaches are unified into a single theory. They study the effect of temperature (at constant P), the effect of pressure (at constant T) and the comined effect of temperature and pressure. **Li *et al*. (2010a**) developed a model for the the size dependent melting temperature of metallic and bimetallic nanowires by considering the contribution of all the surface atoms atoms to the surface area, lattice and surface packing factors and the cross-sectional shape. The melting temperature is a size dependent property, as the size decreases the melting temperature also decreases. The depression in melting

temperature is dramatic in smaller particle size, while smooth for larger size. The model was successful to define the melting temperature for metallic and bimetallic nanowires for the both small large dimensional system.

Li *et al*. (2010b) developed a model on account of size, shape, composition, dimension dependent and surface segregation CE of bimetallic nanosolids. The model was extended to predict the size dependent thermodynamic properties viz. melting temperature, ordering temperature, Curie temperatures, and phase diagram. It was found that the thermodynamic properties of nanosolids not only depend on the atomic percent, the diameter and CE but also depend on size and shape. **Zou *et al*. (2009)** prepared Tin with different size distribution by chemical reduction method and studied the size dependent melting temperature and latent heat of fusion of nanoparticles. Various size dependent melting models were used to examine the size dependent melting properties of Sn nanoparticles and the result showed that the LSM model gives the better knowledge for the melting property. Results obtained from the model showed that the cube root of the latent heat of fusion of Sn nanoparticles is linearly dependent on the reciprocal of the average particle diameter.

Wang *et al*. (2010) studied the high pressure behaviour of β-Ga_2O_3 nanocrystal prepared by chemical method, investigated by angle-dispersive synchrotron x-ray diffraction in a diamond-anvil cell at room temperature. A phase transition occurs, nc-monoclinic β-Ga_2O_3 goes in a phase transition to α-Ga_2O_3. They concluded with a result that the phase-transition pressure and bulk modulus of nc-β-Ga_2O_3 is higher than the bulk counterpart. **Xiong *et al*. (2011a)** calculated the formation enthalpies and Gibbs free energy using the size and shape dependence. It was found that both the formation enthalpy and Gibbs free energy are composition dependent and both of them decrease with particle size. **Xiong *et al*. (2011b)** developed a thermodynamical model based on bond broken rule and the BOLS model account for the size-dependent surface free energy of nanoparticles and nanocavities. It was found that the surfacr free energy of nanoparticles and nanocavities have opposite behaviour with particle size i.e. the Surface free energy decreases with decreasing nanoparticle size, while it increases with the reduction of cavity diameter valid for (D<10nm). **Marqduart *et al*. (2011)** performed high-pressure synchrotron x-ray diffraction experiments on nc-MgO

compressed under both quasi-hydrostatic and non-hydrostatic conditions in a diamond anvil cell.

Safaei (2011) developed a size-dependent model to predict the CE of nanocrystals viz. nanodisks, nanofilms, nanowires and nanoparticles, on considering the effect of the averaged structural and energetic properties of their surface and volume. The formula obtained for the CE of nanocrystal was applied for the melting point of Ag, Si, In and Bi, evaporation temperature of Au and Ag, vacancy formation energy of Au, diffusion activation energy of Au , surface energy of Au, Al and Na, liquid vapour interfacial energy, curie temperature, debye temperature and band gap of Al, Na, Pb, Au, Fe and Si. **Liang (2011)** discussed a simple unified model about the size-dependent elastic modulus and vibration frequency of nanocrystalline metals, ceramics and semiconductors based on the inherent lattice strain and the binding energy change of nanocrystals compared with the bulk crystals and the various nanomaterials are Cu, Ag, Si thin films, nanoparticles, and TiO_2 nanoparticles. **Singh *et al.* (2012)** discussed EOS to study the effect of pressure on volume expansion of nanomaterials. They used only two input parameters for calculations, namely, the bulk modulus and its first pressure derivative. They considered various nanomaterials [Ag (55nm), Ni (20 nm), Cu (80nm) and α-Fe (nanotubes)] [Ge (49 nm), MgO (20nm), Si, CdSe (rock-salt phase) and ZnO] and carbon nanotube (CNT) to determine the effects of pressure on these nanomaterials. **Bhatt and Kumar (2012)** proposed a simple theoretical model to study the size dependence of EOS for nanomaterials. They studied the isothermal compression curve of Ni and Fe for different sizes. On increasing the particle a shift in compression curve is obtained, this demonstrates that the softening of material on increasing particle size. **Chen *et al.* (2013)** investigated the High-pressure strength and plastic properties of nc-TaC. The bulk modulus of nc-TaC is very close to diamond and higher than its bulk counterpart. The yield strength of nc-TaC in plastic deformation starts from ~ 20 GPa and then increases with pressure and reaches a value of ~22 GPa which the highest pressure they reach. **Kumar and Kumar (2013)** discussed a simple thermodynamical analysis of EOS from thermal expansion of nanomaterials. Isothermal compression and pressure dependence of bulk modulus has been studied for different materials.

Bhatt *et al.* (2013) made an effort to find a suitable EOS for nanomaterials. They studied six EOS models viz. Birch-Murnaghan model, Murnaghan model, Kumar model, Vinet model, Ferund and Ignalls model and Tallon model to examin the compression behaviour of thirty one nanomaterials. **Wang *et al*. (2013)** investigated the compression behaviour of nc-TiN for the sizes 16nm, 34nm and 80nm. They found that the bulk modulus of nc-TiN first increases and decreases with a decrease in grain size and also there were no phase transition was during the compression. **Li (2014)** developed a theoretical model to understand the size and shape dependent CE of nanomaterials. It was found that CE of nanoparticles decreases with a decrease in size. **Sharma and Kumar (2014**) developed a simple theoretical model for the size and shape dependent thermoelastic properties of nanomaterials. They observed that the size and shape is very much affected by temperature and so they included temperature and pressure also. They studied the variation of volume and bulk modulus under the effect of shape, size, temperature and pressure. **Ghosh *et al*. (2014)** studied the size and shape dependent structural parameters of ZnO, the apparent change in morphology of nanostructures is linked with the specific changes in various structural parameters. They reported a comprehensive study of size dependent structural parameter of ZnO nanostructure having a wide range of aspect ratio (length/diameter), with increase in size ZnO nanostructure undergoes a shape transition from spherical to rod morphology. **Bhatt *et al*. (2014)** proposed a simple theoretical model to study the effect of size on elastic and thermodynamic properties of nanomaterial. The model was applied to Pb, Fe spherical nanosolid and Au nanowire. **Yan *et al*. (2014)** studied the phase transition and compressibility of nc-Ho_2O_3 under high pressure with help of x-ray diffraction and raman spectroscopy. On increasing the pressure several phase transition occurs. It was found that the bulk modulus of nc-Ho_2O_3 is 10% lower than the reported value of bulk- Ho_2O_3.

Font *et al.* (2015) proposed a mathematical model to study the melting process of spherical Au nanoparticles. They modified the standard model using the Gibbs-Thomson equation to include M.P depression. The difference between the previous work and this model is the difference of densities in liquid and solid phases, new term is included which is a kinetic energy term to balance the energy of the

phase change at interface, which changes the form of equation. Approximate numerical and analytical solutions are studied for the size range 10-100nm to study the melting of particles. They observed that the melting process is slower when they included the density term instead of constant density term. The change is due the extra energy term which is kinetic energy term so they concluded that the density variation effect becomes more important with decreasing particle size. **Li *et al.* (2015)** used a molecular dynamic simulation to study the melting temperature of Ag-Cu. They observed that the melting temperature of core shell nanoparticles is lower than that of the pure Cu nanoparticles.

Singh *et al.* (2015) studied the grain size effects on the volume thermal expansion of nanomaterial. A simple theoretical model was reported to study the size dependence of volume thermal expansion of Nanomaterials for spherical nanoparticles, nanowire and nanofilms. **Sharma and Kumar (2015)** developed a simple theoretical model to study the effect of size for different nanomaterials. They included materials showing hardening, softening, very low effect and no effect. **Qi (2016)** reported a good review of nanoscopic thermodynamics based on the BEM. This model helps us to reproduce a size and shape dependence in a number of physical properties**. Patel *et al.* (2016)** modified the liquid drop model for the size and shape dependent melting temperature of Si and Pb nanoparticles, the shape of nanoparticles was introduced with a new parameter called shape factor. it was found that the particle shape affects the melting temperature of nanoparticles and with the decrease in particle size the melting temperature increases. It was observed that the results obtained with the model were in a good agreement with a experimental data which supports the validity of model.

Bhatt and Kumar (2017) developed a simple theoretical model to study the effect of size, shape, temperature and pressure and used to study the EOS and pressure dependence of lattice parameter of SnO_2 nanomaterial. They used the model to study the compression behaviour at room temperature. **Goyal and Gupta (2017)** proposed a theoretical model to study the thermodynamical properties of nanomaterials for different shapes and sizes. They demonstrated the variation of melting temperature, cohesive energy, Debye temperature, specific heat capacity and

energy band gap with the shape and size of nanomaterials. They observed that the cohesive energy, melting temperature and Debye temperature decreases with a decrease in particle size. Moreover, the energy band gap and specific heat capacity increases with the particle size.

Singh (2018) proposed a model to study the size and shape dependence of the thermal expansion coefficient and specific heat of Ag and Ni nanoparticles for different shapes based on BEM model. He observed that the thermal expansion and specific heat changes with the shape of nanomaterials and maximum for regular tetragon and minimum for spherical shape, cocluded that the thermal expansion and specific heat increases with decreasing the particle size**. Zhang *et al.* (2018)** studied the size and shape dependent melting temperature of nanomaterials. Using an idea for surface atoms and interior atoms affects the melting temperature of materials in a different way, thus they defined an equivalent relationship between the contribution of surface atoms and interior atoms. Based on this definition, a model is proposed for melting temperature through introducing a critical energy storage density of melting which is the sum of the contribution of surface atoms and the interior atoms. Thus, a different theoretical model was developed to define the size effect of melting temperatures of nanomaterials. **Kholiya *et al*. (2019**) reported a simple theoretical model to study the pressure dependence of compressibility for bulk and nc-SnO_2 of different sizes (3,8 and 14nm) using EOS. They demonstrated that the effect of size and pressure on compression, showed the dependency of nanocrystalline size on compression. They found that the compressibility increases with decreasing nanocrystalline size. **Lie *et al*. (2019)** studied the synthesis and high pressure mechanical properties of superhard Rhenium Diboride (ReB_2) and Rhenium Tungsten Diboride ($Re_{0.52}W_{0.48}B_2$). Mechanical properties in situ radial X-ray diffraction was performed under high pressures in a diamond anvil cell. The EOS for n- ReB_2 and n-$RE_{0.52}W_{0.48}B_2$ were measured using hydrostatic volume data measured. They found a small difference in the bulk modulus of n- ReB_2 compared with bulk counterpart, while n-$RE_{0.52}W_{0.48}B_2$ was found incompressible to bulk counterpart. **Chhabra and Kumar (2020)** developed a simple model for the development of size and shape dependent model for magnetic properties from bulk to nanoscale.

A careful review of literature shows that there are several number of experimental studies performed on nanomaterials to understand the effect of size, shape, pressure and temperature for the different properties of nanomaterials. However, the theoretical understandings are lacking. Thus, it is legitimate and may be useful to report a theoretical approach to discuss the properties of nanosolids under the effect of size, shape and pressure, which is an object of present thesis.

Materials and Methods

High pressure and high temperature studies of nanomaterials are our current interest because nanomaterials are very sensitive towards it, so it offers new paths for the investigation of fundamental phenomena and for the elaboration of new materials with new or improved properties.

In this chapter, the simple equations are used to study the effect of pressure, size and shape of nanomaterials. Basically EOS plays an important role to describe the behaviour of materials under the effect of pressure, volume and temperature. An EOS describes how the volume of materials varies and which consequently depends on pressure, temperature, but this definition of EOS is not applicable for nanomaterials. Nanomaterials have different physical and chemical properties comparatively to their bulk counterparts and they strongly depends on size. So the complete EOS for nanomaterials establishes the relationship between state variables like pressure, volume, temperature and size. If an adequate knowledge of an EOS is available, it can be used to understand the behaviour of nanomaterials under the different thermodynamic conditions.

3.1 Birch Model

Different models of EOS have been reported, some of these are reviewed below. Birch proposed Eularian finite theory of strain which is known as Birch Murnaghan EOS **(Anderson, 1995)**. Birch's original derivation was based on Murnaghan's theory of finite strain. In the theory of the finite strain, the expression for the strain components , referred to the strained state are as follows, (u, v, w) are the components of the displacement (x, y, z) are the Cartesian coordinates after the displacement of a point.

$$E_{xx} = \frac{\partial u}{\partial x} - \frac{1}{2}\left[\left(\frac{\partial u}{\partial x}\right)^2 + \left(\frac{\partial v}{\partial y}\right)^2 + \left(\frac{\partial w}{\partial z}\right)^2\right] \quad (3.1)$$

$$E_{yz} = \frac{1}{2}\left(\frac{\partial v}{\partial z} - \frac{\partial w}{\partial y}\right) - \left[\frac{\partial u}{\partial y}\frac{\partial u}{\partial z} + \frac{\partial v}{\partial y}\frac{\partial v}{\partial z} + \frac{\partial w}{\partial y}\frac{\partial w}{\partial z}\right] \quad (3.2)$$

In case of hydrostatic strain of a medium of isotropic or cubic symmetry, the strain degenerate into a single component.

$$E = \frac{\partial u}{\partial x} - \frac{1}{2}\left(\frac{\partial u}{\partial x}\right)^2 = \frac{\partial v}{\partial y} - \frac{1}{2}\left(\frac{\partial v}{\partial y}\right)^2 = \frac{\partial w}{\partial z} - \frac{1}{2}\left(\frac{\partial w}{\partial z}\right)^2 \quad (3.3)$$

The relation between strain E with density ρ or Volume V is

$$\frac{V_0}{V} = \frac{\rho}{\rho_0} = (1 - 2E)^{3/2} = (1 + 2f)^{3/2} \quad (3.4)$$

The strain energy expressed as

$$\Psi = af^2 + bf^3 + cf^4 + \ldots\ldots\ldots \quad (3.5)$$

where a, b, c…….. are constants and used to represent the functions of temperature. From the thermodynamic relation we can obtain the relation between volume and hydrostatic pressure is

$$P = -\left(\frac{\partial \Psi}{\partial t}\right) \quad (3.6)$$

Where Ψ is the Helmholtz free energy, and V denotes volume per unit mass. Then the pressure is,

$$P = \left(\frac{\partial f}{\partial v}\right)\left(\frac{\partial \Psi}{\partial f}\right)_T = (3V_0)^{-1}(1 + 2f)^{5/2}(2af + 3bf^2 + \ldots\ldots\ldots) \quad (3.7)$$

Using the notation used by (Birch 1947), now the pressure written as

$$P = 3B_0\,(1+2f)^{5/2}\left(1 - \frac{fD_3}{3B_0\rho}\ldots.\right) \quad (3.8)$$

In terms of density

$$P = \frac{3}{2}\left[\left(\frac{\rho}{\rho_0}\right)^{\frac{7}{3}} - \left(\frac{\rho}{\rho_0}\right)^{\frac{5}{3}}\right]\left\{1 - \xi\left[\left(\frac{\rho}{\rho_0}\right)^{\frac{2}{3}} - 1\right] + \cdots\right\} \quad (3.9)$$

ξ was defined by Birch and its value is

$$\xi = \frac{3}{4}(4 - B_0') \quad (3.10)$$

on neglecting higher order terms and using this equation we get

$$P = \frac{3}{2}\left[\left(\frac{\rho}{\rho_0}\right)^{\frac{7}{3}} - \left(\frac{\rho}{\rho_0}\right)^{\frac{5}{3}}\right]\left\{1 - \frac{3}{4}(4 - B_0')\left[\left(\frac{\rho}{\rho_0}\right)^{\frac{2}{3}} - 1\right] + \cdots\right\} \quad (3.11)$$

Or

$$P = \frac{3}{2}\left[\left(\frac{\rho}{\rho_0}\right)^{\frac{7}{3}} - \left(\frac{\rho}{\rho_0}\right)^{\frac{5}{3}}\right]\left\{1 + \frac{3}{4}\,(B_0' - 4)\left[\left(\frac{\rho}{\rho_0}\right)^{\frac{2}{3}} - 1\right] + \cdots\right\} \quad (3.12)$$

The Bulk Modulus corresponding to Eq. (3.12)

$$B = \frac{B_0}{2}\left[7\left(\frac{V_0}{V}\right)^{-\frac{7}{3}} - 5\left(\frac{V_0}{V}\right)^{-\frac{5}{3}}\right] + \frac{3}{8}B_0(B_0' - 4)\left[9\left(\frac{V}{V_0}\right)^{-3} - 14\left(\frac{V}{V_0}\right)^{-\frac{7}{3}} + 5\left(\frac{V}{V_0}\right)^{-\frac{5}{3}}\right] \quad (3.13)$$

Here, P is the pressure, B is the bulk modulus and V/V_0 is the relative change in volume. On taking $B_0' = 4$ above equation reduces in the following form:

$$B = \frac{3}{2}B_0'\left[\left(\frac{V_0}{V}\right)^{\frac{7}{3}} - \left(\frac{V_0}{V}\right)^{\frac{5}{3}}\right] \quad (3.14)$$

This equation is known as Birch equation.

3.2 Tallon Model

Tallon (1998) proposed a model for the isobaric variations of volume and thermal expansion coefficient with temperature and used the concept of modified Gruneisen parameter g defined as

$$g_{MP} = -V_0\left[\frac{\partial lnM}{\partial V}\right]_P \quad (3.15)$$

where V_0 is the volume at room temperature T_0 and at atmospheric pressure. M represents the elastic constant, above equation gives the basis to study the temperature dependence of M at a constant pressure. Integrating Eq. (3.15) at constant pressure we get

$$M(T,P) = M(T_0, P)\exp\left\{g_{MP}\frac{\Delta_P V}{V_0}\right\} \quad (3.16)$$

Where $\Delta_P V$ is the isobaric volume change

$$\Delta_P V = V(T,P) - V(T_0,P) \quad (3.17)$$

When we put isobaric bulk modulus B in place of M of Eq. (3.16) we get

$$B(T,P) = B(T_0, P)\exp\left\{g_{MP}\frac{\Delta_P V}{V_0}\right\} \quad (3.18)$$

Above equation gives an isobaric variation of bulk modulus with temperature. Since αB is temperature independent, so the temperature dependence of α is given by the temperature dependence of B. Thus,

$$\alpha(T,P) = \alpha(T_0, P)\exp g_{BP}\left[\frac{V(T,P)-V(T_0,P)}{V_0}\right] \quad (3.19)$$

on integrating

$$E_l\left[g_{BP}\frac{V(T,P)}{V_0}\right] = E_l\left[g_{BP}\frac{V(T_0,P)}{V_0}\right] - \alpha(T_0,P)exp\left[-g_{BP}\frac{V(T_0,P)}{V_0}\right](T-T_0) \quad (3.20)$$

Where $E_l(x)$ is the exponential integral.This equation is at zero isobar so for the sake of notation, $\alpha(T_0, 0)$ and $\frac{V(T,0)-V(T_0,0)}{V_0(T^0,0)}$ denoted here by α_0 and $\frac{\Delta_P V}{V_0}$

Using the approximation, this gives

$$1-\left[\frac{g_{BP}^2}{g_{BP}-1}\right]\alpha_0(T-T_0) = \exp\left\{-g_{BP}\frac{\Delta_P V}{V_0}\right\}\left\{\frac{1+\Delta_P V}{V_0}\right\}^{-1} = \alpha_0\frac{V_0}{\alpha V} \quad (3.21)$$

Integrating above equation with respect to temperature gives

$$\frac{\Delta_P V}{V_0} = -\left[\frac{g_{BP}-1}{g_{BP}^2}\right]\ln\left\{1-\left(\frac{(g_{BP}^2)}{(g_{BP}-1)}\right)\alpha_0(T-T_0)\right\} \quad (3.22)$$

The values of g_{BP} are not available for all the materials so the model is not very useful.

3.3 Kumar and Upadhyay Model

Using thermodynamic analysis Kumar and Upadhyay (1994) developed a model, as discussed below

$$\delta_T = -\frac{1}{\alpha B_T}\left[\frac{\partial B_T}{\partial T}\right]_P \quad (3.23)$$

where α is the coefficient of volume thermal expansion and defined as

$$\alpha = \frac{1}{V}\left[\frac{\partial V}{\partial T}\right]_P \quad (3.24)$$

and B_T is the isothermal bulk modulus and defined as

$$B_T = -V\left[\frac{\partial P}{\partial V}\right]_T \quad (3.25)$$

One of the well known Maxwell thermodynamic identity is

$$B_T\left[\frac{\partial \alpha}{\partial P}\right]_T = \frac{1}{B_T}\left[\frac{\partial B_T}{\partial T}\right]_P \quad (3.26)$$

Above Eq. (3.23), (3.25) and (3.26) gives the following relation

$$\frac{d\alpha}{\alpha} = \delta_T\left(\frac{dV}{V}\right) \quad (3.27)$$

On integrating, this gives

$$\frac{\alpha}{\alpha_0} = \left(\frac{V}{V_0}\right)^{\delta_T} \quad (3.28)$$

Where V_0 and α_0 are the volume and thermal expansion coefficient at atmospheric pressure (P=0) and temperature condition. For solids like NaCl type structure $V= 2r^3$ where r is an interatomic separation.

Thus Eq.(3.28) can be rewritten as

$$\frac{\alpha}{\alpha_0} = \left(\frac{r}{r_0}\right)^{3\delta_T} \quad (3.29)$$

From the definition of thermal expansion coefficient α

$$\frac{\alpha}{\alpha_0} = \frac{1}{3}ar \quad (3.30)$$

From Eq. (3.29) and (3.30),yields

$$\frac{dr}{dT} = \frac{1}{3}\alpha_0 \frac{r^{x+1}}{{r_0}^x} \quad (3.31)$$

Where $x = 3\delta_T$

On integrating above Eq. gives

$$\int_{r_0}^{r} \frac{dr}{r^{x+1}} = \frac{1}{3}\frac{\alpha_0}{{r_0}^x}\int_{T_0}^{T} dT = \frac{1}{3}\frac{\alpha_0}{{r_0}^x}(T - T_0) \quad (3.32)$$

Gives

$$r(T) = r_0\left[\frac{1}{1-\delta_T\alpha^0(T-T^0)}\right] \quad (3.33)$$

Eq. (3.33) known as kumar and Upadhyay model, and from Eq. (3.15) following equation may be obtained

$$\alpha(T) = \alpha_0\left[\frac{1}{1-\delta_T\alpha^0(T-T^0)}\right] \quad (3.34)$$

Above equations give the temperature dependence of r(T) and α(T).

3.4 He and Yan Model

He and Yan proposed a model for the temperature dependence of interatomic sepeartion.

$$\delta_T = -\left(\frac{1}{\alpha B_T}\right)\left(\frac{\partial B_T}{\partial T}\right)_P \quad (3.35)$$

where B_T and α are the bulk modulus and thermal expansion coefficient respectively and defined as

$$\alpha = \frac{1}{V}\left[\frac{\partial V}{\partial T}\right]_P \quad (3.36)$$

and

$$B_T = -V\left[\frac{\partial P}{\partial V}\right]_T \quad (3.37)$$

He and Yan assumed that the dependence of α on temperature is quadratically.

$$\alpha(T) = \alpha_0 + \alpha_0'(T-T_0) + \left(\frac{1}{2}\right)\alpha_0''(T-T_0)^2 \quad (3.38)$$

α_0, α_0' and α_0'' are zero first and second order temperature derivative of α at T_0. using a well known thermodynamic expression αB_T = constant, gives

$$\delta_T = \left(\frac{1}{\alpha^2}\right)\left(\frac{\partial \alpha}{\partial T}\right)_P \quad (3.39)$$

this Eq.(3.39) gives the following results

$$\alpha_0' = \left(\frac{\partial \alpha}{\partial T}\right)_p = \delta_T \alpha_0^2 \quad (3.40)$$

$$\alpha_0'' = \left(\frac{\partial^2 \alpha}{\partial T^2}\right)_P = 2\,\delta_T^2 \alpha_0^3 \quad (3.41)$$

The another assumption is that the Anderson Gruneisen parameter δ_T is independent of temperature (T). Thus Eq. (3.38) can be written as

$$\alpha(T) = \alpha_0 + \alpha_0^2 \delta_T(T-T_0) + \alpha_0^3 \delta_T^2(T-T_0)^2 \quad (3.42)$$

on Substituting the value of α in Eq. (3.35), we get the following relation

$$\frac{dB_T}{B_T} = -\delta_T[\alpha_0 + \alpha_0^2 \delta_T(T-T_0) + \alpha_0^3 \delta_T^2(T-T_0)^2]dT \quad (3.43)$$

Gives

$$B_T(T = B_0 \exp\left[-\alpha_0 \delta\tau(T - T_0)\left\{1 + \left(\frac{1}{2}\right)\alpha_0 \delta\tau(T - T_0) + \left(\frac{1}{3}\right)\alpha_0{}^2 \delta\tau^2 (T - T_0)^2\right\}\right] \quad (3.44)$$

Substituting

$$\frac{dV}{V} = [\alpha_0 + \alpha_0{}^2 \delta\tau(T - T_0) + \alpha_0{}^3 \delta\tau^2 (T - T_0)^2]dT \quad (3.45)$$

$$\frac{V}{V_0} = \exp\left[-\alpha_0 (T - T_0)\left\{1 + \left(\frac{1}{2}\right)\alpha_0 \delta\tau(T - T_0) + \left(\frac{1}{3}\right)\alpha_0{}^2 \delta\tau^2 (T - T_0)^2\right\}\right] \quad (3.46)$$

This is a isobaric EOS which can be used to find out the values of V/V_0 from room temperature to melting temperature along an isobar.

However, on considering the relation $(V/V_0) = (r/r_0)^3$ Eq. (3.46) converted in the following form:

$$r = r_0 \exp\left[\left(\frac{1}{3}\right)\alpha_0 (T - T_0)\left\{1 + \left(\frac{1}{2}\right)\alpha_0 \delta\tau(T - T_0) + \left(\frac{1}{3}\right)\alpha_0{}^2 \delta\tau^2 (T - T_0)^2\right\}\right] \quad (3.47)$$

the above equation is referred as He and Yan relation.

3.5 Murnaghan EOS

Equation of state from pressure dependence of bulk modulus, which depends linearly on the pressure **(Murnaghan, 1994).**

$$B = B_0 + B_0' P \quad (3.48)$$

Bulk modulus is defined as

$$B = -V\frac{dP}{dV} \quad (3.49)$$

$$\frac{dV}{V} = \frac{dP}{B + B_0' P} \quad (3.50)$$

On integrating Eq. (3.50), we get

$$\ln(V) = -\frac{1}{B_0'}\ln\left(1 + \frac{B_0'}{B_0} P\right) \quad (3.51)$$

or

$$\ln\left(\frac{V_0}{V}\right) = -\frac{1}{B_0'} ln\left(1 + \frac{B_0'}{B_0} P\right) \quad (3.52)$$

or $\frac{V}{V_0} = \left(1 + \frac{B_0'}{B_0} P\right)^{-\frac{1}{B_0'}}$ (3.53)

or $P = \frac{B_0}{B_0'} [exp\left\{-B_0' ln\left(\frac{V}{V^0}\right)\right\} - 1]$ (3.54)

Eq. (3.54) is known as Murnaghan EOS.

Theory of the EOS based on thermodynamic analysis was reported by **Kumar (1995).**

High pressure research demonstrates that the product of α (coefficient of volume thermal expansion) and B (bulk modulus) remains constant under the effect of pressure,

αB = constant (3.55)

on partial differentiating Eq. (3.55), we get

$\alpha \left(\frac{\partial v}{\partial B}\right) + B \left(\frac{\partial \alpha}{\partial V}\right) = 0$ (3.56)

which gives

$\delta_T = \frac{V}{\alpha}\left(\frac{\partial \alpha}{\partial V}\right) = -\frac{V}{B}\frac{\partial B}{\partial V}$ (3.57)

where δ_T is known as Anderson Gruneisen parameter. At fixed temperature we can write above equation as

$\frac{\partial B}{B} = -\delta_T \frac{\partial V}{V}$ (3.58)

Integrating Eq. (3.11) with limits $B = B_0$ when $V = V_0$ gives:

$\frac{B}{B_0} = \left(\frac{V}{V_0}\right)^{-\delta_T}$ (3.59)

As $B = -V\left(\frac{\partial P}{\partial V}\right)$ (3.60)

Eq. (3.12) gives

$-\frac{V}{B_0}\left(\frac{\partial P}{\partial V}\right) = \left(\frac{V}{V_0}\right)^{\delta_T}$ (3.61)

or

$\frac{dV}{V^{\delta_T+1}} = -\frac{-1}{B_0 V_0^{\delta_T}} dP$ (3.62)

From Eq. (3.57) $\delta_T = \left(\frac{dB}{dP}\right)_T = B_0'$

Integrating Eq. (3.15) for a limit $V = V_0$ at $P = P_0$ gives

$$P = \frac{B_0}{B_0'}\left[\exp\left\{-B_0' ln\left(\frac{V}{V_0}\right)\right\} - 1\right] \quad (3.63)$$

Eq. (3.16) is also known as Murnaghan EOS.

In this section, we study an EOS from thermal expansion of nanomaterials. When a material is heated it will expand and when cooled down it will contract for a given temperature.

The coefficient of thermal expansion α is defined as:

$$\alpha = \frac{1}{V}\left(\frac{dV}{dT}\right)_P \quad (3.64)$$

Prakash (2005) determined α by using molecular dynamic simulation for single wall CNTs, which is given as

$$\alpha = a + bT + cT^2 \quad (3.65)$$

Where, a, b and c are constants. Writing Eq. (3.18) in form of a initial boundary condition, i.e. $\alpha = \alpha_0$ for $T = T_0$.

$$\alpha = a + b\,(T-T_0) + c(T-T_0)^2 \quad (3.66)$$

or

$$\alpha = \alpha_0 + \alpha_0'(T-T_0) + \alpha_0''(T-T_0)^2 \quad (3.67)$$

where α' and α'' are related to δ_T **(He and Yan, 2001)**

$$\alpha_0' = \alpha_0^2 \delta_T \quad (3.68)$$

$$\alpha_0'' = \alpha_0^3 \delta_T^2 \quad (3.69)$$

Now, Eq.(3.19) written as

$$\alpha = \alpha_0 + \alpha_0^2 \delta_T (T-T_0) + \alpha_0^3 \delta_T^2 (T-T_0)^2 \quad (3.70)$$

Eq. (3.23) is true provided that α depends on T quadratically. However, considering the higher terms of Eq.(3.23) may replace the error on the temperature dependence of α. So it is necessary to consider the accurate form of Eq.(3.23).

$\alpha = \alpha_0 + \alpha_0^2\delta_T(T\text{-}T_0) + \alpha_0^3\delta_T^2(T\text{-}T_0)^2 +$ ----------∞ (3.71)

or

$\frac{\alpha}{\alpha_0} = [1 - \alpha_0\delta_T(T - T_0)]^{-1}$ (3.72)

From the definition of volume thermal expansion α , using Eq. (3.17) above equation reduced to

$\frac{V}{V_0} = [1 - \alpha_0\delta_T(T - T_0)]^{-1/\delta_T}$ (3.73)

The thermal pressure P_{th} is defined as **(Anderson, 1995)**

$P_{th} = \alpha_0 B_0(T\text{-}T_0)$ (3.74)

Thus, Eq.(3.24) written as

$\frac{V}{V_0} = \left[1 - \frac{\delta_T}{B_0}P\right]^{-1/\delta_T}$ (3.75)

Or $P_{th} = \frac{B_0}{\delta_T}\left[1 - \left(\frac{V}{V_0}\right)^{-\delta_T}\right]$ (3.76)

When applied pressure is not zero then Eq. (3.27) is transformed as

$P_{th} - P = \frac{B_0}{\delta_T}\left[1 - \left(\frac{V}{V_0}\right)^{-\delta_T}\right]$ (3.77)

And when P_{th}=0, Eq. (3.28) written as

$P = \frac{B_0}{\delta_T}\left[1 - \left(\frac{V}{V_0}\right)^{-\delta_T}\right]$ (3.78)

Using well known approximation $\delta_T = B_0'$ **(Anderson 1995), Eq.**(3.28) read as

$P = \frac{B_0}{B_0'}\left[1 - \left(\frac{V}{V_0}\right)^{-B_0'}\right]$

Or

$P = \frac{B_0}{B_0'}\left[\exp\left\{-B_0' ln\left(\frac{V}{V_0}\right)\right\} - 1\right]$ (3.79)

which is also known as Murnaghan EOS.

Thus, Murnaghan EOS may be derived in different ways.

3.2 Effect of Size and Shape on EOS

Qi (2005, 2016) proposed a model for the CE of nanoparticles (E_{Tot}). According to this model if the total atoms of nanosolid is denoted as n, and number of surface atoms is denoted as N, so the number of interior atoms were denoted as (n-N). Let E_0 be the CE per atom for the bulk materials, then the contribution to the interior atoms to the CE is E_0 (n-N). Since half of the bonds of each surface atoms are the dangling bonds so the contribution of each surface atom to the CE of nanosoild is equal to $E_0/2$.

E_{Tot} is the sum of the contributions of surface atoms and interior atoms, which has been formulated as:-

$$E_{Tot} = E_0(n - N) + \frac{1}{2}E_0N \quad (3.80)$$

Or

$$E_P = E_b\left(1 - \frac{N}{2n}\right) \quad (3.81)$$

Where E_p is the CE per mole of nanosolid, which is written as

$$E_P = \frac{\text{AvEtot}}{n} \quad (3.82)$$

Where, A_v is the Avagadro constant

E_b is the CE per mole of the corresponding bulk material ($E_b = AE_0$).

It is well known that both the CE and the elastic moduli are the parameters to define the rigidity or bond strength of materials. **Kumar and Kumar (2010)** reported that the effect of size on bulk modulus may be defined as

$$B_{0n} = B_{0b}\left(1 - \frac{N}{2n}\right) \quad (3.83)$$

Where B_{0n} and B_{0b} are the bulk modulus of nanomaterials and bulk material respectively.

Now our aim is to compute N/n for the different shapes of nanomaterials viz. film, dodecahedral, icosahedral, wire, spherical, octahedral and tetrahedral. For spherical nanosolid, having diameter D and its volume is $\pi D^3/6$ and the atomic volume can be given by $\pi d^3/6$, where d is the atomic diameter. Then the total number of atoms n is defined as the ratio of the volume of the nanoslolid to the volume of atom i.e. n=

$(\pi D^3/6)/(\pi d^3/6) = D^3/d^3$. The surface area of nanosolid is πD^2 and the contribution of each surface atom to the surface area of the nanosolid is the area of the great circle i.e. $N= (\pi D^2)/(\pi d^2/4)$ and simplified into the form $N/2n = 2d/D$

So for spherical nanosolid, the bulk modulus may be defined as

$$B_{0n} = B_{0b}\left(1 - \frac{2d}{D}\right) \quad (3.84)$$

For others shapes we similary find the N/n ratio which is given in table 4.1

3.5 Effect of temperature on EOS

Nanomaterials are very sensitive towards tempaerature as like pressure and size. So the effect of temperature is also included.

As the thermal pressure P_{th} is defined by **(Anderson, 1995).**

$$\left(\frac{\partial P_{th}}{\partial T}\right)_V = \alpha B \quad (3.85)$$

Where α and B is the coefficient of volume thermal expansion and the bulk modulus respectively, and T is the absolute temperature. Using the Hilderbrand approximation **(Born and Huang, 1954),** on integrating above Eq.(3.85) we get the following relation

$$P_{th} = \int_{T_0}^{T} (\alpha B)\mathrm{d}T \quad (3.86)$$

or

$$P_{th} = \alpha_0 B_0 (T-T_0) \quad (3.87)$$

This is the effect of temperature on EOS.

Now to develop the final EOS for the nanomaterials we include all the effects, effect of size, effect of pressure and effect of temperature. we get the following relation.

$$P = -\frac{B_{0b}}{B'_{0n}}\left(1 - \frac{N}{2n}\right)\left[1 - \left(\frac{V}{V_0}\right)^{-B'_{0n}}\right] + \alpha_{0n} B_{0n} (T-T_0) \quad (3.88)$$

Eq. (3.88) is the EOS for nanomaterials.

Now we have to find the following relations for different shapes, for that we have to compute N/n to find B_{0n} for different nanosolids which is given in Table 4.1

Film:

$$P = -\frac{B_{0b}}{B'_{0n}}\left(1-\frac{0.666d}{h}\right)\left[1-\left(\frac{V}{V_0}\right)^{-B'_{0n}}\right] + \alpha_{0n}B_{0n}(T-T_0) \quad (3.89)$$

Dodecahedral:

$$P = -\frac{B_{0b}}{B'_{0n}}\left(1-\frac{0.898d}{a}\right)\left[1-\left(\frac{V}{V_0}\right)^{-B'_{0n}}\right] + \alpha_{0n}B_{0n}(T-T_0) \quad (3.90)$$

Icosahedral:

$$P = -\frac{B_{0b}}{B'_{0n}}\left(1-\frac{1.323d}{a}\right)\left[1-\left(\frac{V}{V_0}\right)^{-B'_{0n}}\right] + \alpha_{0n}B_{0n}(T-T_0) \quad (3.91)$$

Wire:

$$P = -\frac{B_{0b}}{B'_{0n}}\left(1-\frac{1.323d}{L}\right)\left[1-\left(\frac{V}{V_0}\right)^{-B'_{0n}}\right] + \alpha_{0n}B_{0n}(T-T_0) \quad (3.92)$$

Spherical:

$$P = -\frac{B_{0b}}{B'_{0n}}\left(1-\frac{2d}{D}\right)\left[1-\left(\frac{V}{V_0}\right)^{-B'_{0n}}\right] + \alpha_{0n}B_{0n}(T-T_0) \quad (3.93)$$

Octahedral:

$$P = -\frac{B_{0b}}{B'_{0n}}\left(1-\frac{2.449d}{a}\right)\left[1-\left(\frac{V}{V_0}\right)^{-B'_{0n}}\right] + \alpha_{0n}B_{0n}(T-T_0) \quad (3.94)$$

Tetrahedral:

$$P = -\frac{B_{0b}}{B'_{0n}}\left(1-\frac{4.898d}{a}\right)\left[1-\left(\frac{V}{V_0}\right)^{-B'_{0n}}\right] + \alpha_{0n}B_{0n}(T-T_0) \quad (3.95)$$

This gives the theory of the EOS with a effect of size, shape, pressure and temperature. In the present thesis, we used above relations to study the size and shape effect on nanomaterials under varying conditions of pressure. We used different materials for this purpose. The results obtained are given in chapter 4 along with the available experimental data.

Results and Discussion

Chapter 4 RESULTS AND DISCUSSION

In this chapter, we analyzed the results obtained from the various formulations as reported in chapter 3. We discussed different models for the EOS and and we carry forward the Murnaghan EOS. By help of Murnaghan EOS we study the compression behaviour of nanomaterials and the effect of pressure, size and shape. The input parameters which are required for the present work are given in Table 4.2. There are a number of models proposed to know thermodynamical behaviour of nanomaterials. There are different theories related to the MEOS Eqs. (3.54) (3.63) and (3.78) which are studied in present thesis. However the derivations are well known for higher pressure ranges **(Kumar, 1995)** for bulk materials. As Murnaghan neglects the higher terms and assumed the bulk modulus depend linealy on pressure given by Eq. (3.48).

Theoretical as well as experimental works on EOS suggested that the Murnaghan EOS Eq. (3.48) can be used to study the compression behaviour of nanomaterials and also the effect of pressure, size and shape. Thus Eq. (3.88) is the final equation of our present thesis which gives the effect of size, shape and pressure, further Eq. (3.89) to (3.95) is the MEOS for different shapes and values used there were from table 4.1. we have performed our studies on the materials viz. MgO (20nm), ZnO_2 (3.1nm), WC (25nm), n-ReB_2 (40nm), n-$ReWB_2$ (30nm), TiN (18nm), TiN (34nm), TiN (80nm), α-Ga_2O_3 (14nm), β- Ga_2O_3 (14nm), Ho_2O_3 (14nm) because of some experimental data are available on these materials so the comparison is also possible. Firstly in present chapter we compare experimental data with our results comes from model then we studied the nanomaterials for the different sizes and shapes. The studies has been made at room temperature for all the materials considered in the present work.

Table 4.1: N/n values for different shapes of nanosolids **(Bhatt and kumar, 2017)**

S.No.	Shape of Nanosolid	N/n
1.	Film	1.333d/h
2.	Dodecahedral	1.796d/a
3.	Icosahedral	2.646d/a
4.	Wire	2.666d/L
5.	Spherical	4d/D
6.	Octahedral	4.898d/a
7.	Tetrahedral	9.797d/a

Table 4.2: List of the materials with the parameter used n present thesis

S.No	NANOMATERIAL	B_{0n}	B'_{0n}	REFERENCES
1.	MgO (20nm)	185.5		Marqduart *et al.* (2011) Rekhii *et al.* (2002)
2.	MgO (11nm)	146.7	4.0	Marqduart *et al.* (2011)
3.	ZnO_2 (3.1nm)	174	4.71	Chen *et al.* (2009)
4.	WC (25nm)	452	1.25	Lin *et al.* (2009)
5.	ReB_2 (50nm)	326	4.4	Lei *et al.* (2019)
6.	$Re_{0.52}W_{0.48}B_2$ (120nm)	349	1.7	Lei *et al.* (2019)
7.	TiN (16nm)	320	4	Wang *et al.* (2010)
8.	TiN (34nm)	338	4	Wang *et al.* (2010)
9.	TiN (80nm)	287	4	Wang *et al.* (2010)
10.	α-Ga_2O_3 (14nm)	333	4	Wang *et al.* (2009)
11.	β-Ga_2O_3 (14nm)	228	4	Wang *et al.* (2009)
12.	Ho_2O_3 (14nm)	164	4	Yan *et al.* (2014)

We have used Eq. (3.88) to compute the behaviour of nanomaterials at different sizes, for different shapes i.e. film, dodecahedral, icosahedral, wire, spherical, octahedral and tetrahedral, we have used Eq. (3.89) to Eq. (3.95) respectively. The compression behaviour for MgO (20nm) at room temperature has been reported in **Fig. 1** along with experimental data, the experimental data was reported by **Marqduart *et al.* (2011)** and there is a good agreement between theory and experimental data. Further we study the compression behaviour for different sizes of MgO (11nm, 40nm, 60nm, 80nm and 100nm). The results are reported in **Fig. 2-6** is the combined figure reported for the different sizes of MgO (11nm, 20nm and 100nm). An interesting thing to be noted is that the compression behaviour of 20nm and 100nm collapse together and seems one line. Overall we found a shift in a isotherm from the size 11nm to 100nm. We are reporting these results in absence of experimental data. After that we also studied the pressure dependence of V/V_0 for different shapes reported in **Fig. 7.** We studied all nanomaterials at room temperature. Now for the nanomaterial ZnO_2 (3.1nm), we studied the compression behaviour for the particle size 3.1nm was reported in **Fig. 8**. After that we studied in a similar fashion firstly for different sizes ZnO_2 (40nm, 60nm, 80nm) and plotted in **Fig. 9-11** respectively, then we plotted a combined pressure dependence of V/V_0 for different shapes viz. 3.1nm, 10nm and 90nm and we observed a shift in isotherm with increase in size from 3.1nm to 90nm and reported in **Fig. 12**. Finally, we study the shape effect in compression behaviour of ZnO_2 (3.1nm) and reported in **Fig.13.**

Pressure dependence of V/V_0 for different sizes of WC has been plotted in the **Fig.14-17**. In **Fig. 14** WC (25nm) plotted the compression behaviour with an experimental data, as given by **Lin *et al.* (2009).** Our model is in good agreement with experimental data. Shape effect is also studied and reported in **Fig.18.** Now coming on another material Rhenium Dibroide (ReB_2) and Rhenium tungsten diboride ($Re_{0.52}W_{0.48}B_2$), **Lei *et al.* (2019)** studied both the materials together. **Fig. 19** represents the compression behaviour of n- ReB_2 (40nm) with experimental data after that **Fig. 20-25** represents for the different size at last **Fig. 26** reported is reported for the different shapes.

In **Fig. 27**, the combined plot for the ReB_2 (40nm) and $Re_{0.52}W_{0.48}B_2$ (30nm) and the isotherm curve clearly defines the hardness increased by adding W. For $Re_{0.52}W_{0.48}B_2$ (30nm). The pressure dependence of V/V_0 for different sizes is plotted in **Fig. 28-31**. Plot for the different shapes is represented by the **Fig. 32**.

For TiN (16nm, 34nm and 80nm), the plots of pressure dependence of V/V_0 has been depicted with experimental data and represented by the **Fig. 33-35** respectively. Experimental data was given by **Wang *et al.* (2010)**. Our results are in a good agreement with experimental data. The compression curve for the different sizes is represented by **Fig. 36-40**. **Fig. 41** reported the shape effect of TiN (80nm).**Wang *et al.* (2010)** studied the high pressure of β-Ga_2O_3 along with this also studied the combined compression curve for α- Ga_2O_3. From **Fig.42-46** represents the compression curve of α- Ga_2O_3 for different sizes after that **Fig. 47** represents the compression curve for the different shapes of α- Ga_2O_3. The combined plot for β-Ga_2O_3 and α- Ga_2O_3 is reprented in **Fig. 48. Fig. 48** represents the compression curve of β-Ga_2O_3 (14nm) with experimental data carried from **Wang *et al.* (2010).** From **Fig. 50-53** represents the pressure dependence of V/V_0 for different sizes for β-Ga_2O_3. The compression curve of β-Ga_2O_3 for the different shapes is represented by **Fig.54**. The results calculated are in good agreement with experimental data. For Ho_2O_3 (14nm), the compression curve with experimental data given by **Yan *et al.* (2014)** was represented by **Fig. 55**. The pressure dependence of V/V_0 for the different sizes is represented from the **Fig. 56-59** and the **Fig. 60** represents the compression curve for the different shapes.

We observe that for the nanomaterials studied in the present thesis a shift in isotherm is found as we increase size. As the pressure is increased we get the more compressed form of particle. Also, we see that for different shapes of nanomaterials viz. film, dodecahedral, icosahedral, wire, spherical, octahedral and tetrahedral. The largest shift in isotherm is observed in case of film and the least in tetrahedral. Since bulk modulus is inversely proportional to compressibility so it is quite evident that tetrahedral nanosolid are least compressible and followed by the order octahedral, spherical, wire, icosahedral, dodecahedral and film respectively.

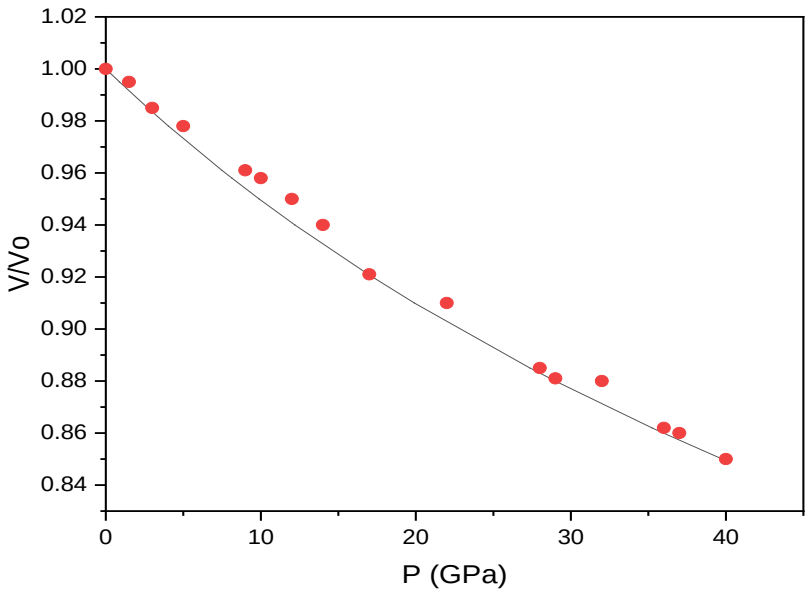

Figure 1: Pressure dependence of V/V_0 for MgO (20nm) using Eq. (3.88), • demonstrate the experimental data (**Marqduart *et al.*, 2011)**

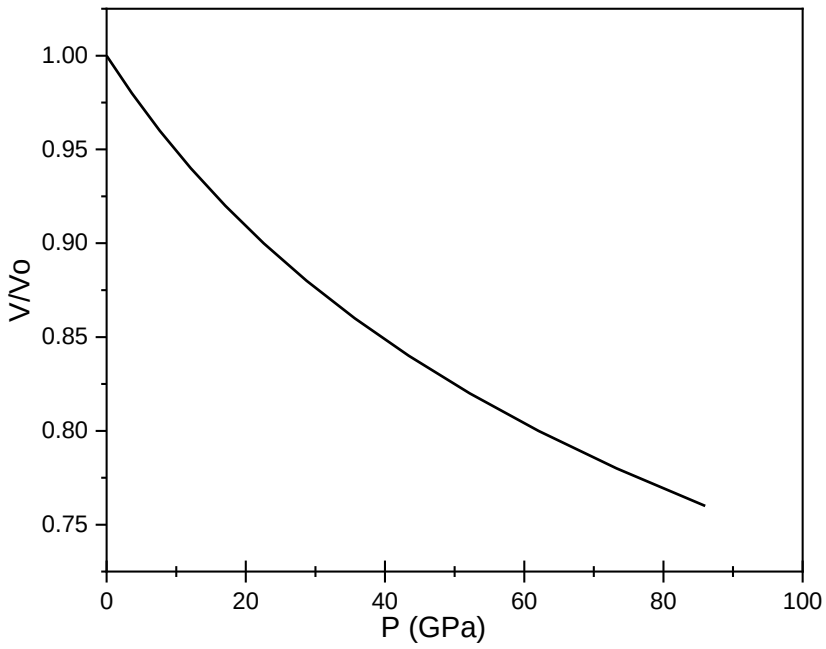

Figure 2: Pressure dependence of V/V_0 for MgO (11nm) by using Eq. (3.88)

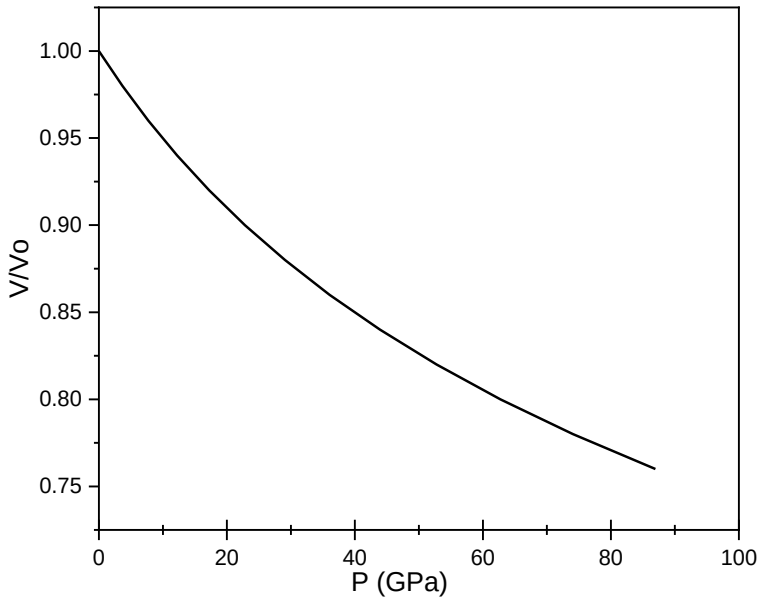

Figure 3: Pressure dependence of V/V_0 for MgO (40nm) using Eq. (3.88)

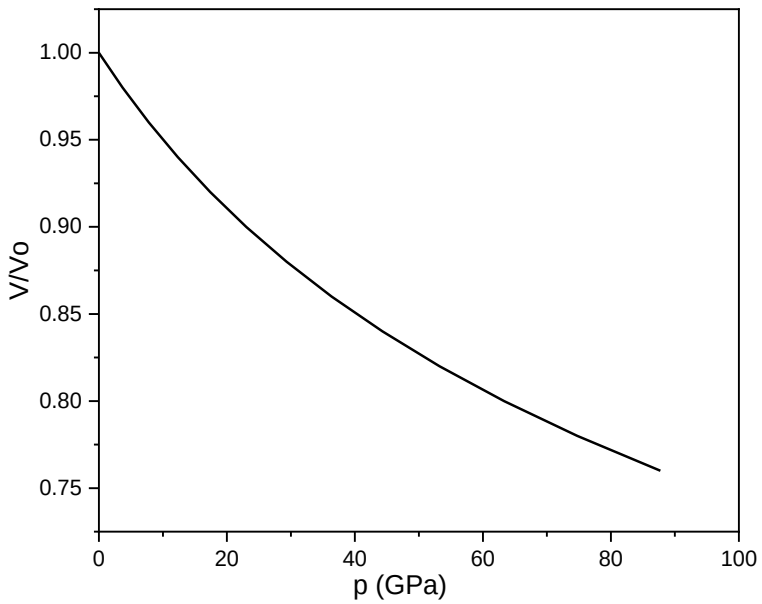

Figure 4: Pressure dependence of V/Vo for MgO (60nm) using Eq. (3.88)

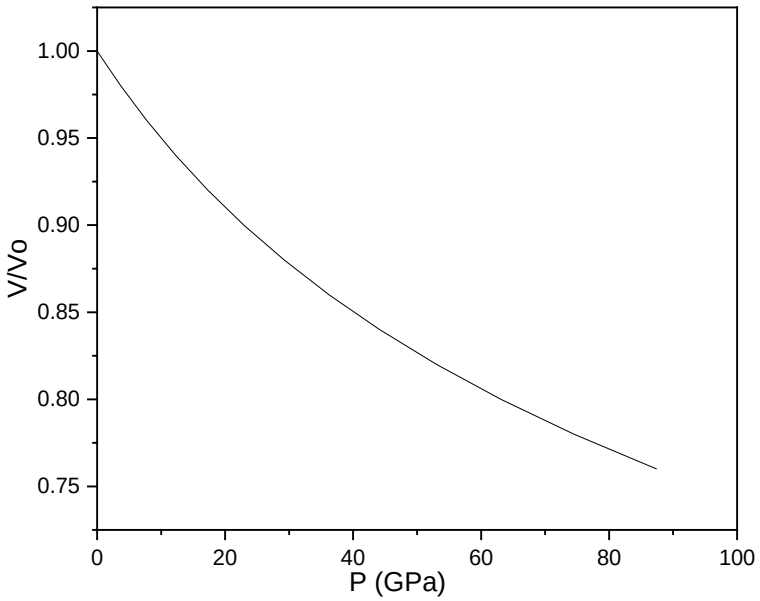

Figure 5: Pressure dependence of V/V_0 for MgO (80nm) by using Eq. (3.88)

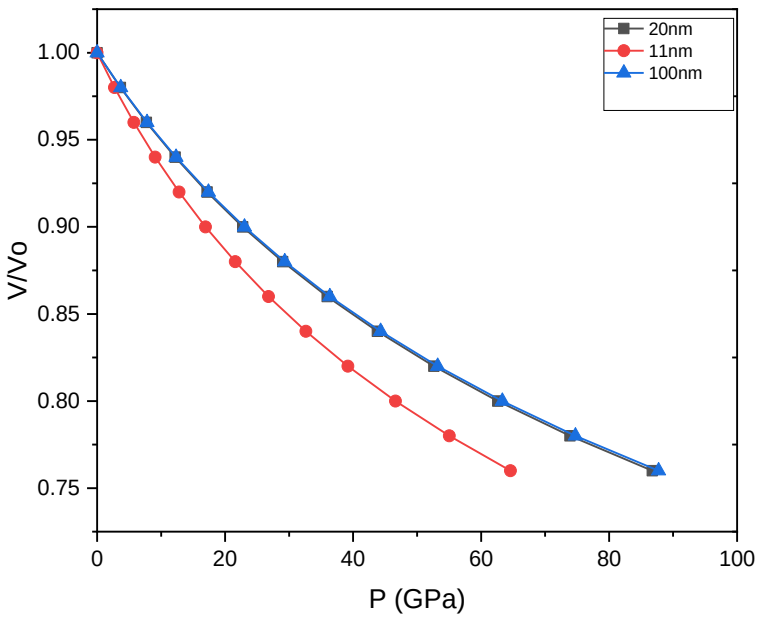

Figure 6: Pressure dependence of V/V_0 for different sizes of MgO (spherical), using Eq. (3.88)

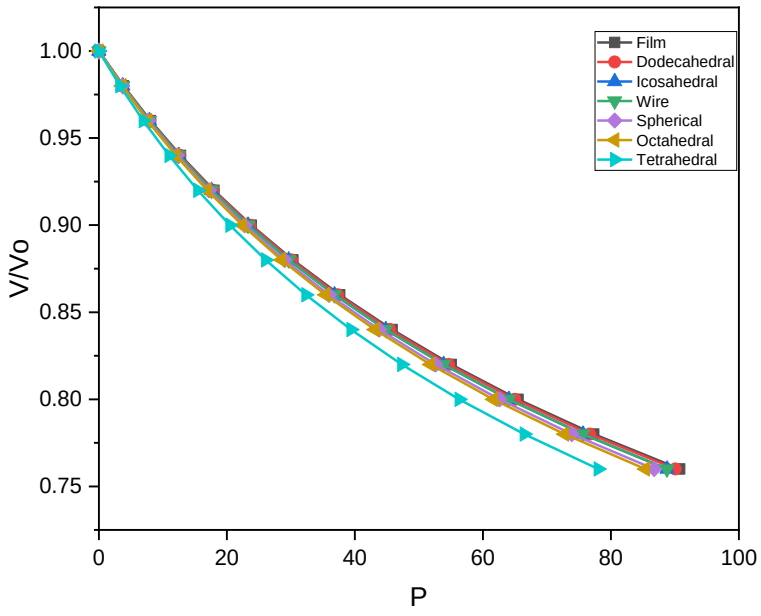

Figure 7: Pressure dependence of V/V_0 for different shapes of MgO (20nm), using Eqs. (3.89-3.95)

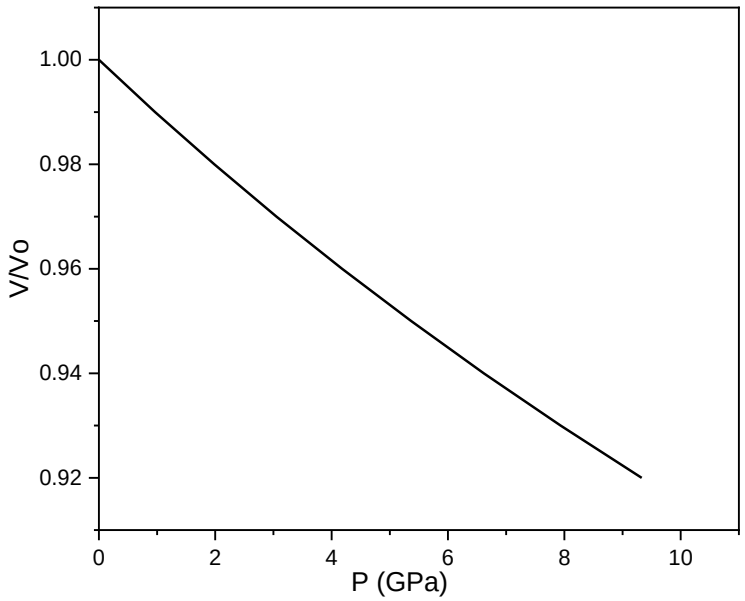

Figure 8: Pressure dependence of V/V_0 for ZnO_2 (3.1nm), using Eq. (3.88)

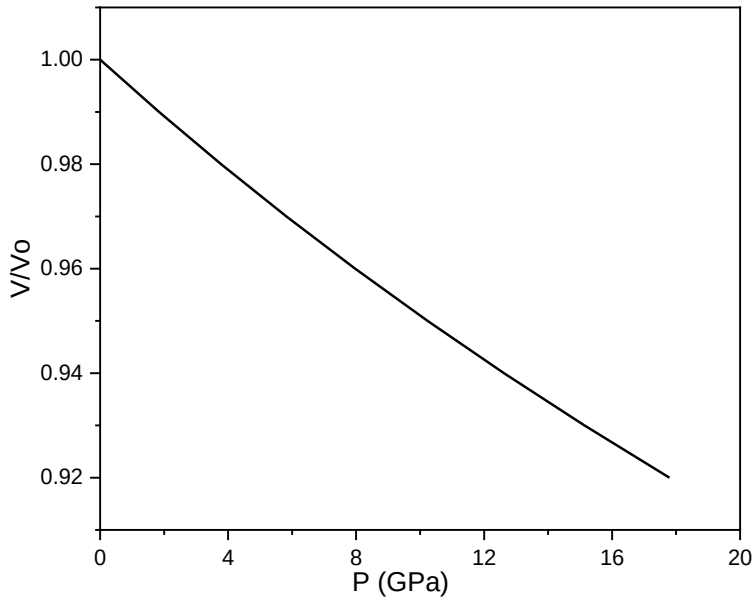

Figure 9: Pressure dependence of V/V_0 for ZnO_2 (40nm) using Eq. (3.88)

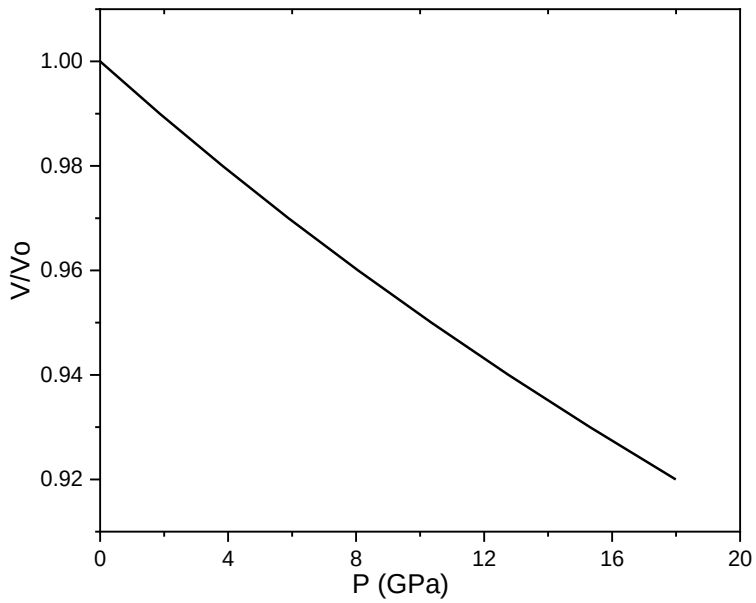

Figure 10: Pressure dependence of V/V_0 for ZnO_2 (60nm) using Eq. (3.88)

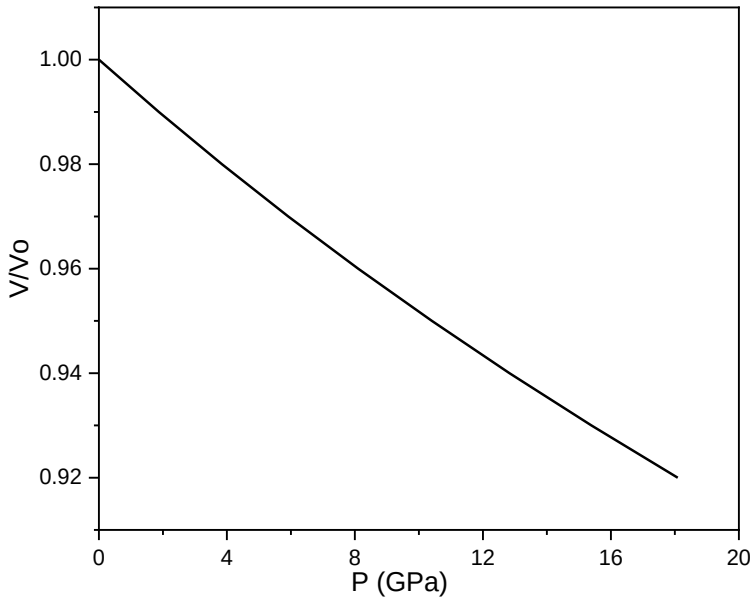

Figure 11: Pressure dependence of V/V_0 for ZnO_2 (80nm) using Eq. (3.88)

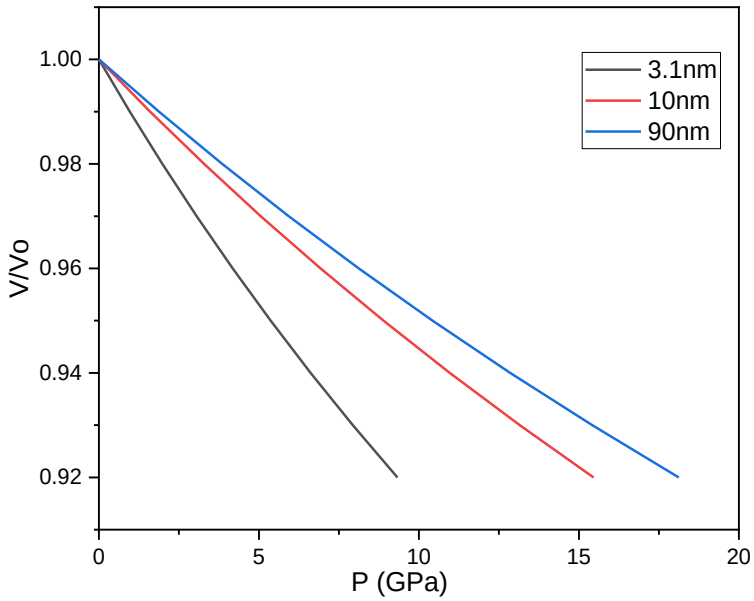

Figure 12: Pressure dependence of V/V_0 for different sizes of ZnO_2 (spherical) by using Eq. (3.88)

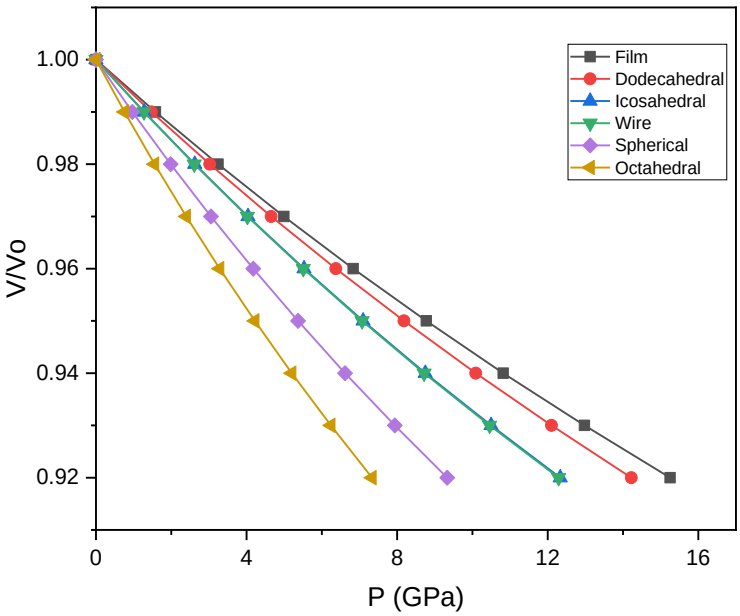

Figure 13: Pressure dependence of V/V_0 for different shapes of ZnO_2 (3.1nm), using Eqs. (89-95)

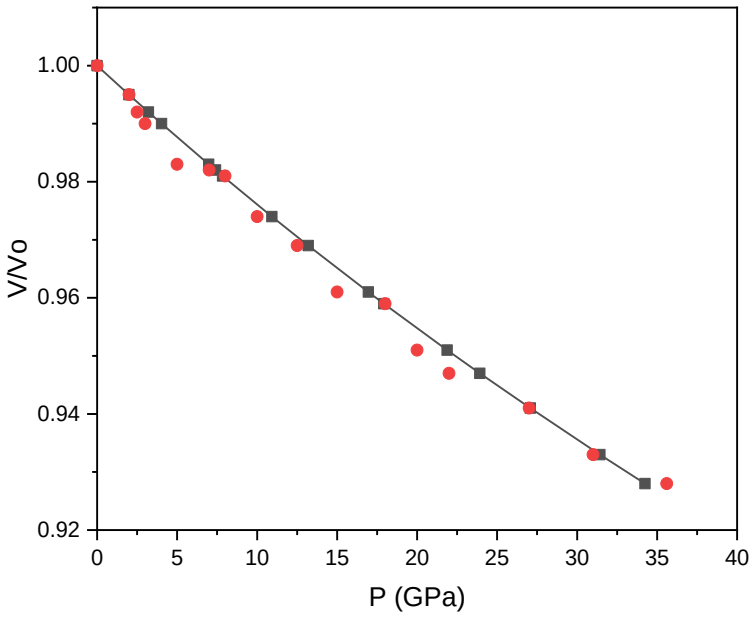

Figure 14: Pressure dependence of V/V_0 for n-WC (25nm), using Eq. (3.88), • demonstrates experimental data **(Lin *et al.* 2009)**

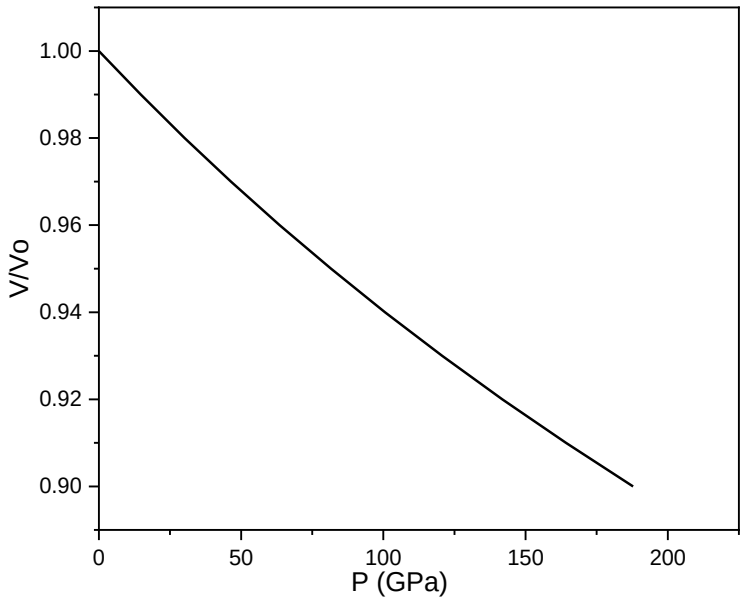

Figure 15: Pressure dependence of V/V_0 for n-WC (50nm), using Eq. (3.88)

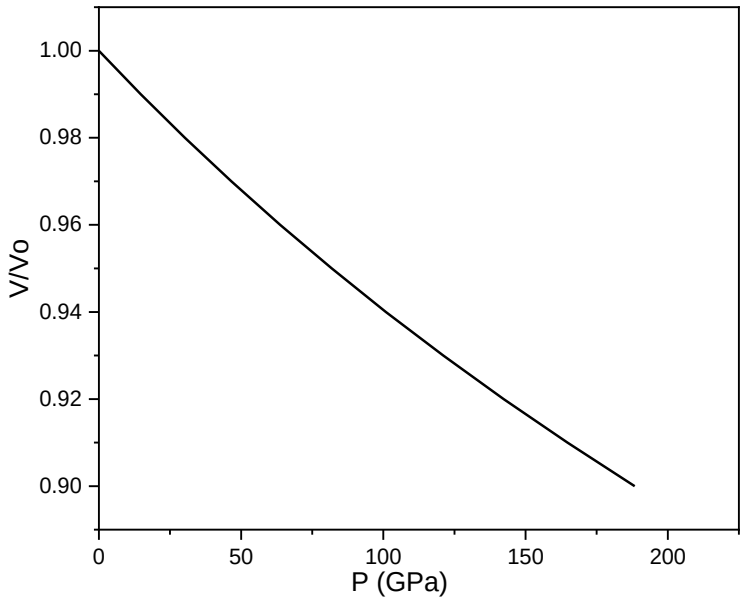

Figure 16: Pressure dependence of V/V_0 for WC (75nm), using Eq. (3.88)

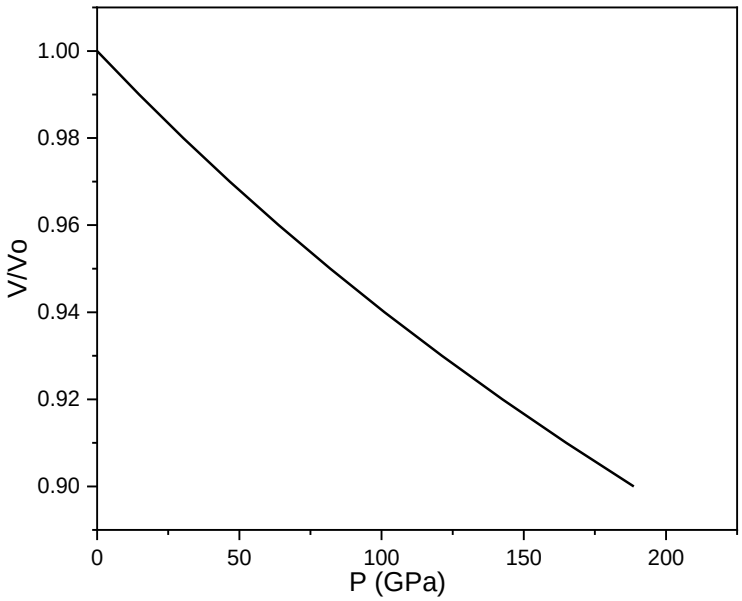

Figure 17: Pressure dependence of V/V_0 for n-WC (100nm), using Eq. (3.88)

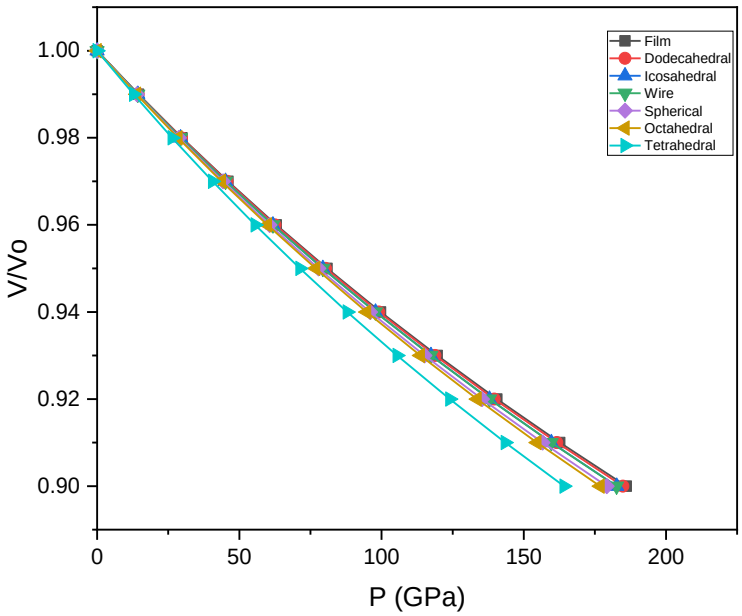

Figure 18: Pressure dependence of V/V_0 for different shapes of n-WC (25cm), using Eqs. (3.89-3.95).

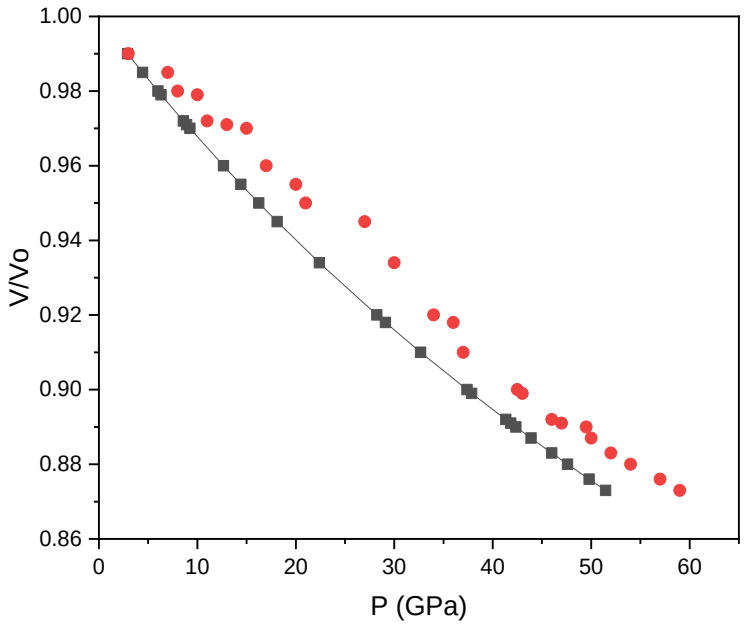

Figure 19: Pressure dependence of V/V_0 for n-ReB_2 (40nm) using Eq. (3.88), • demonstrate experimental data **(Lei *et al.* 2019)**

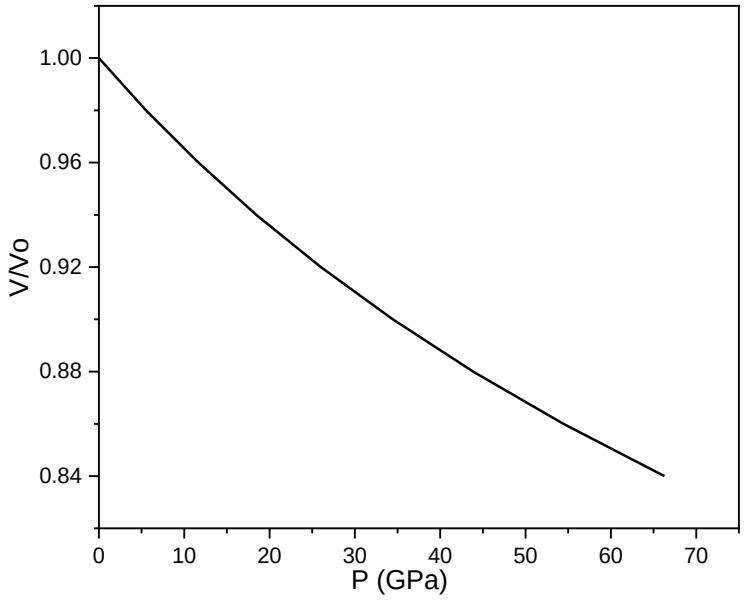

Figure 20: Pressure dependence of V/V_0 for n-ReB_2 (20nm), using Equation (3.88)

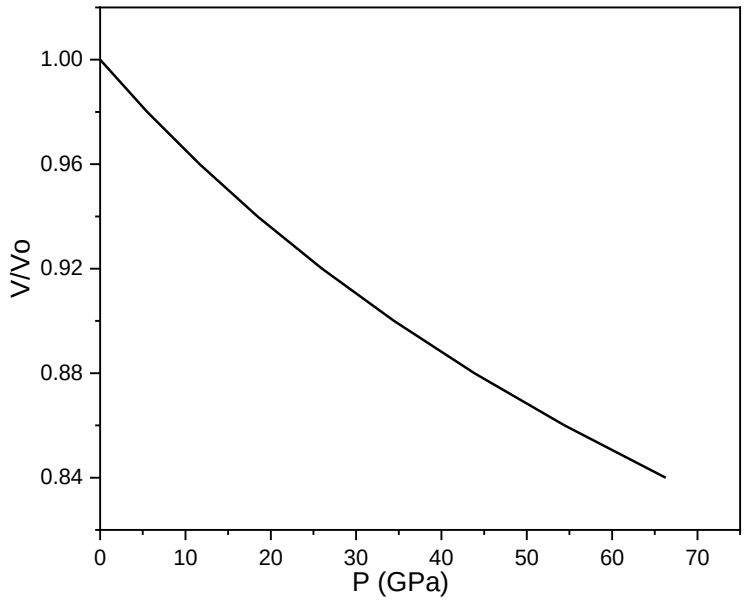

Figure 21: Pressure dependence of V/V_0 for n-ReB_2 (20nm), using Eq. (3.88)

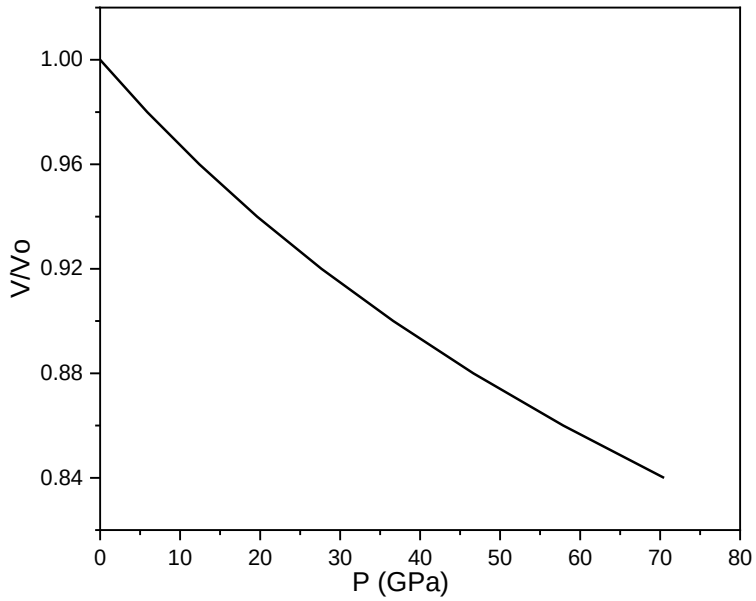

Figure 22: Pressure dependence of V/V_0 for n-ReB_2 (40nm), using Eq. (3.88)

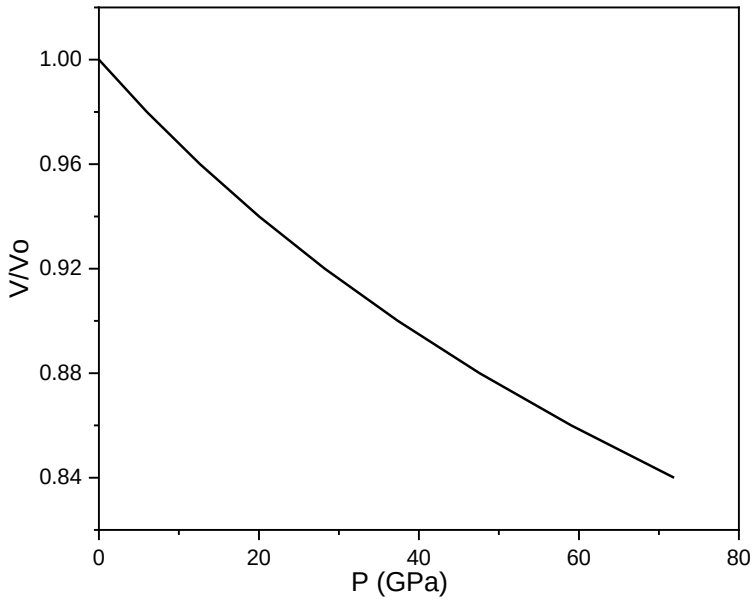

Figure 23: Pressure dependence of V/V_0 for n-ReB_2 (60nm), using Eq. (3.88)

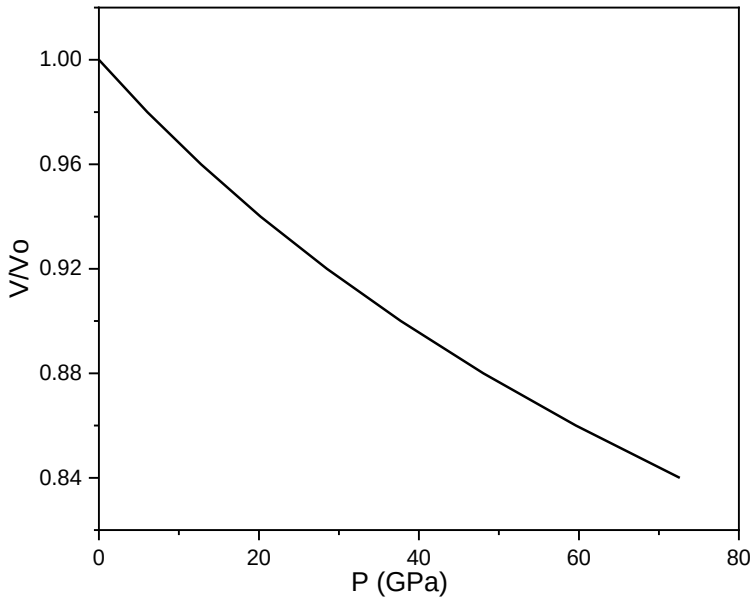

Figure 24: Pressure dependence of V/V_0 for n-ReB_2 (80nm), using Eq. (3.88)

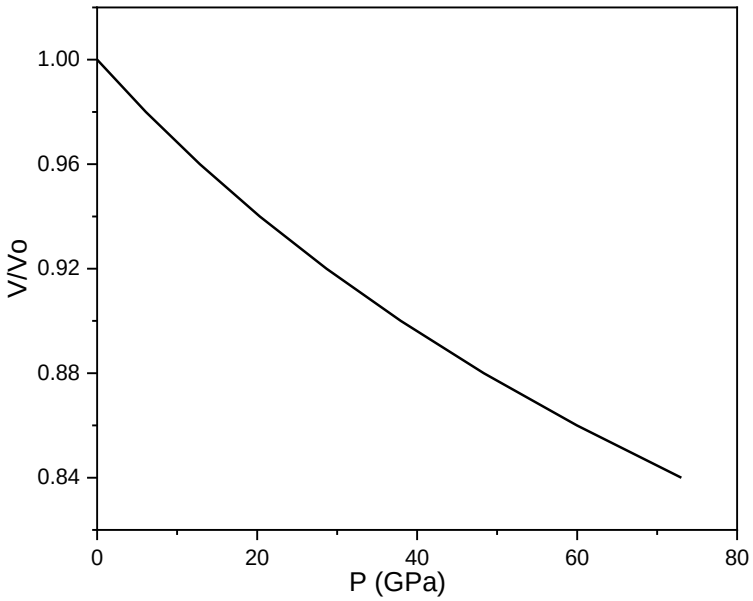

Figure 25: Pressure dependence of V/V_0 for n-ReB_2 (100nm), using Eq. (3.88)

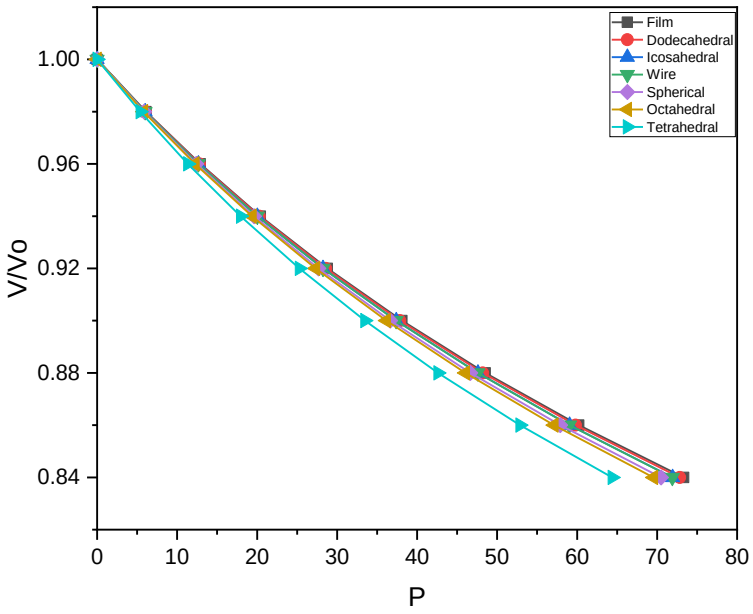

Figure 26: Pressure dependence of V/V_0 for n-ReB_2 (40nm), using Eqs. (3.89-3.95)

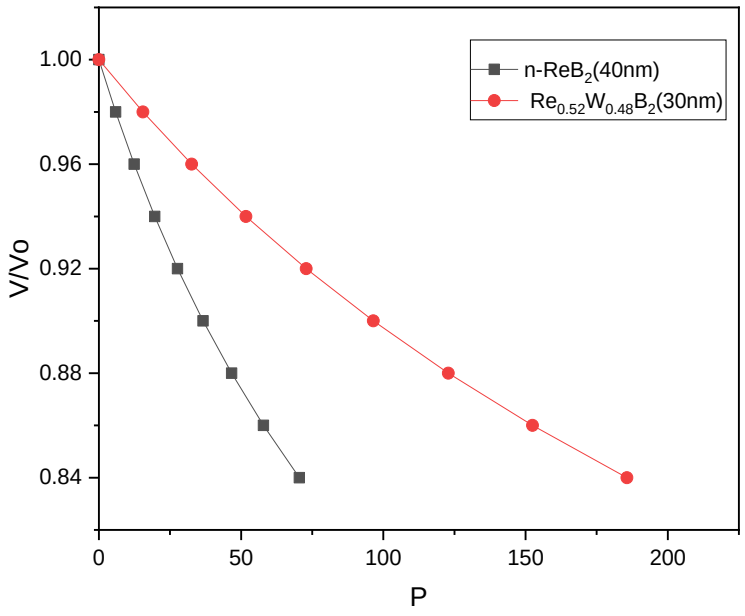

Figure 27: Pressure dependence of V/V_0 for n-ReB_2 (40nm) and n-$Re_{0.52}W_{0.48}B_2$ (30nm), using Eq. (3.88)

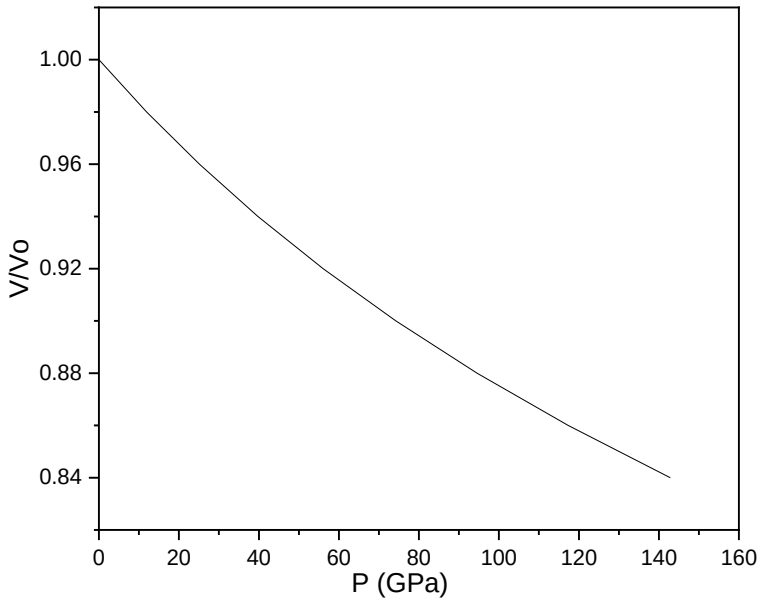

Figure 28: Pressure dependence of V/V_0 for $Re0_{.52}W_{0.48}B_2$ (10nm) using Eq. (3.88)

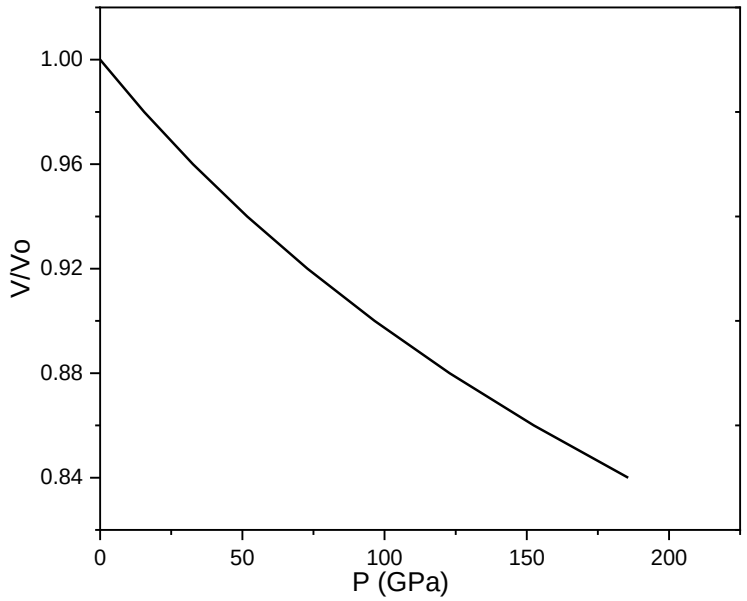

Figure 29: Pressure dependence of V/V_0 for n- $Re_{0.52}W_{0.48}B_2$ (30nm), using Eq. (3.88)

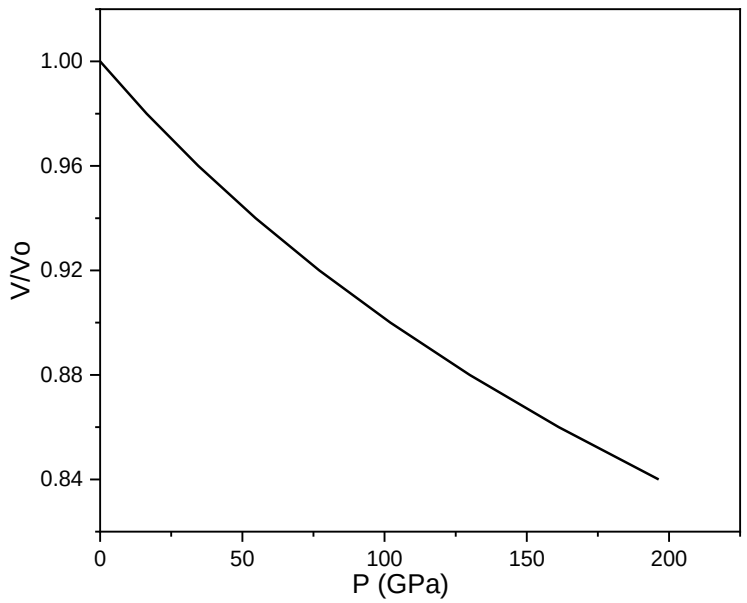

Figure 30: Pressure dependence of V/V_0 for n- $Re_{0.52}W_{0.48}B_2$ (60nm), using Eq. (3.88)

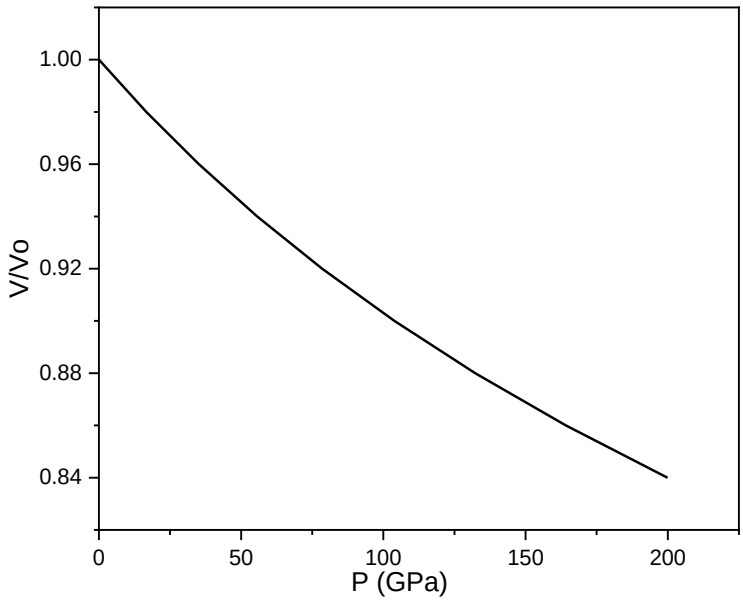

Figure 31: Pressure dependence of V/V_0 for n- $Re_{0.52}W_{0.48}B_2$ (90nm), using Eq. (3.88)

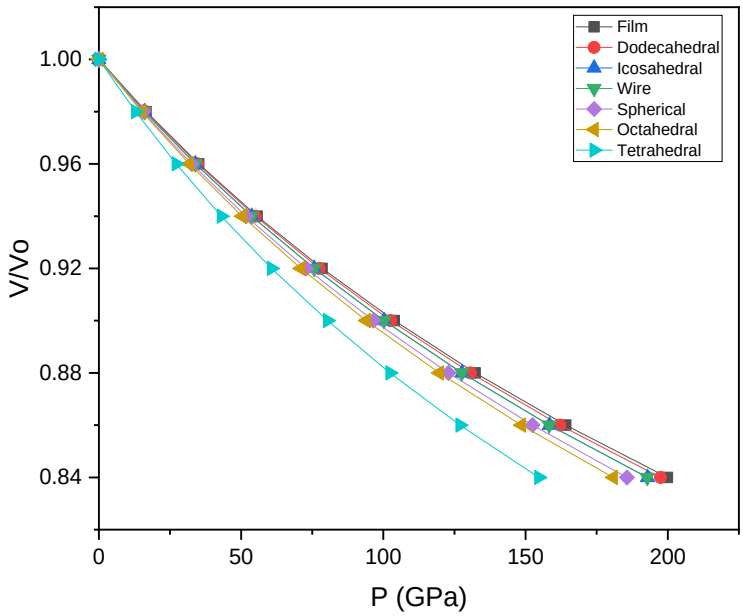

Figure 32: Pressure dependence of V/V_0 for different shapes of n- $Re_{0.52}W_{0.48}B_2$ (30nm) using Eqs. (3.89-3.95)

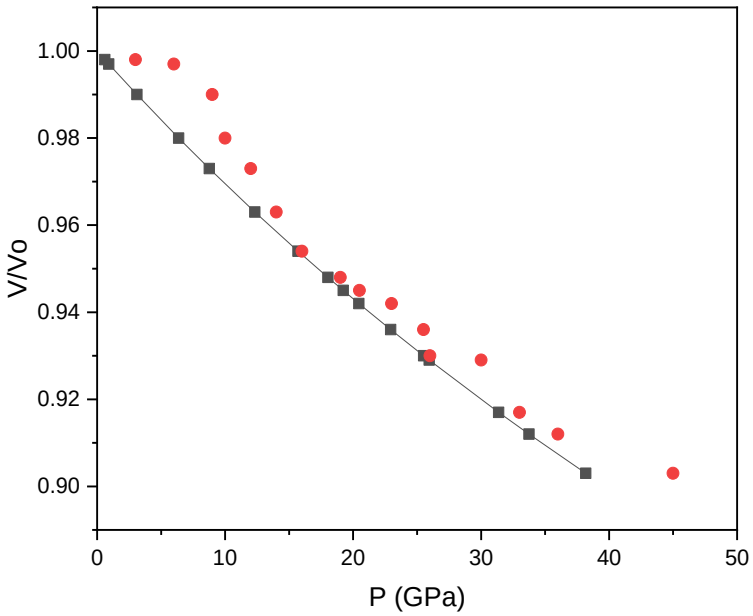

Figure 33: Pressure dependence of V/V_0 for different shapes of n-TiN (16nm) using Eq. (3.88), • demonstrates the experimental data **(Wang *et al.* 2010)**

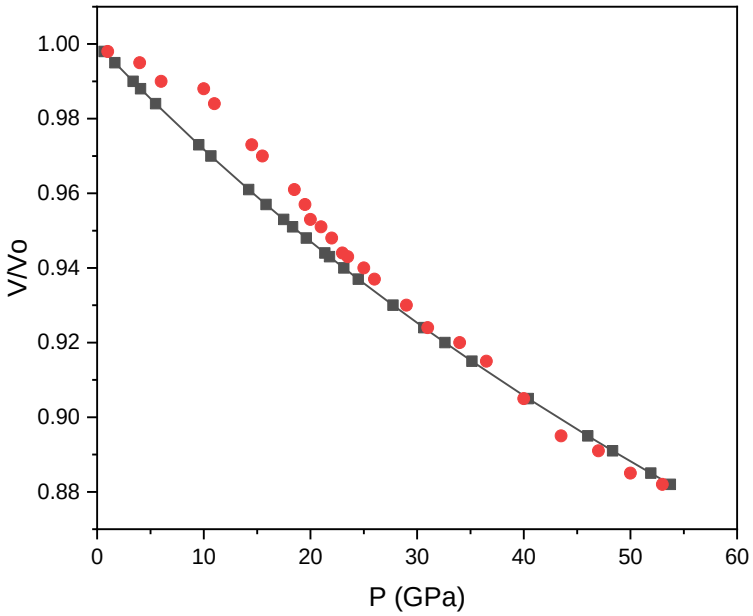

Figure 34: Pressure dependence of V/V_0 for different shapes of n-TiN (34nm) using Eq. (3.88), • demonstrates the experimental data **(Wang *et al.* 2010)**

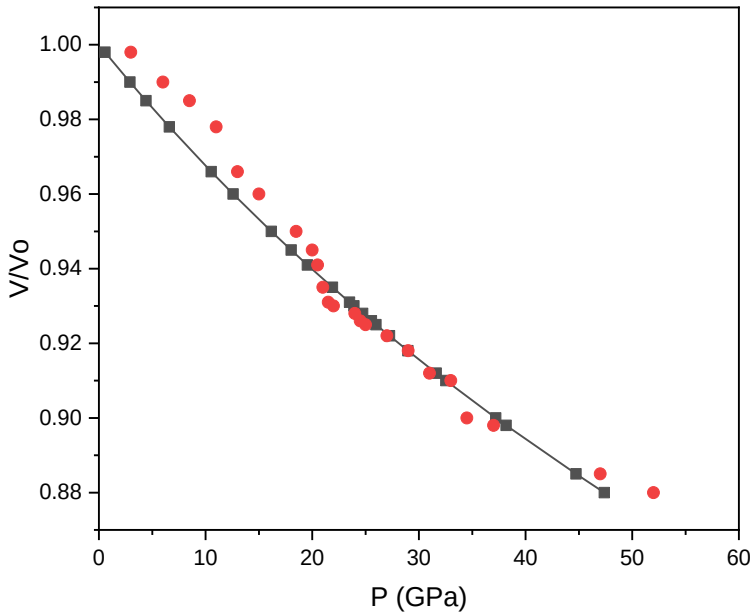

Figure 35: Pressure dependence of V/V_0 for different shapes of n-TiN (80nm) using Eq. (3.88), • demonstrates the experimental data **(Wang *et al.* 2010)**

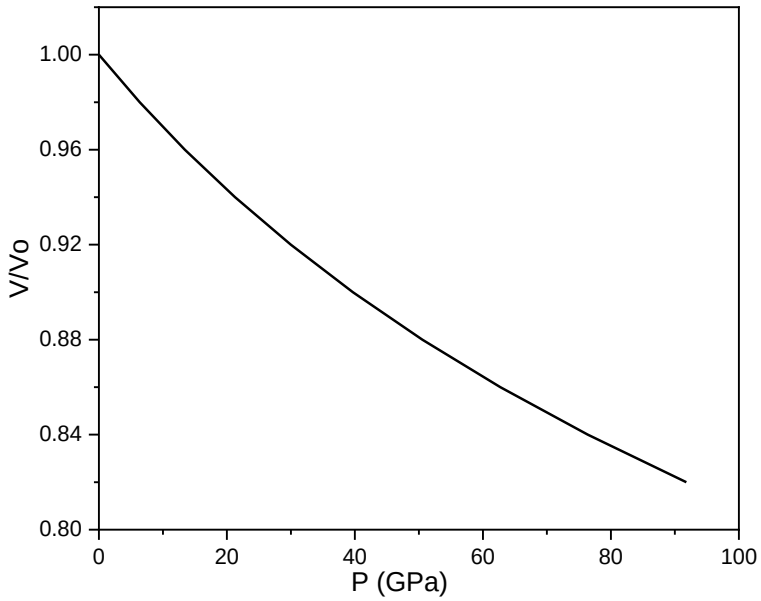

Figure 36: Pressure dependence of V/V_0 for n-TiN (16nm), using Eq. (3.88)

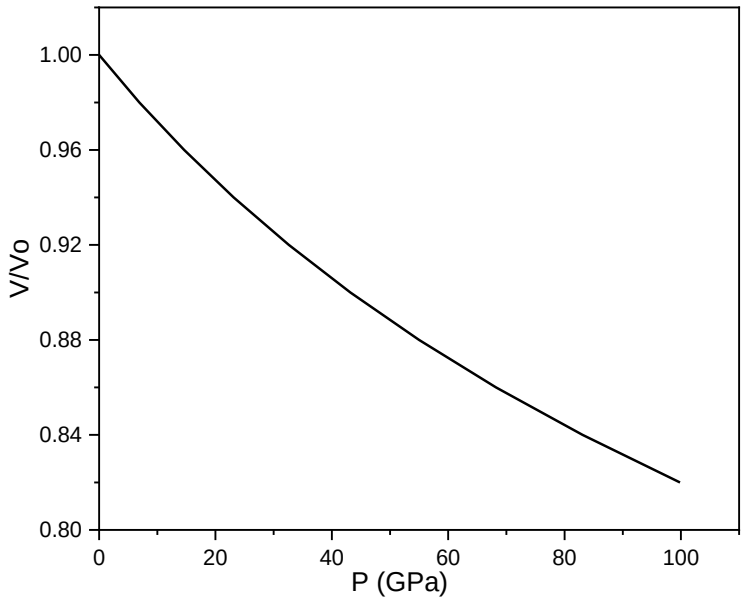

Figure 37: Pressure dependence of V/V_0 for n-TiN (34nm), using Eq. (3.88)

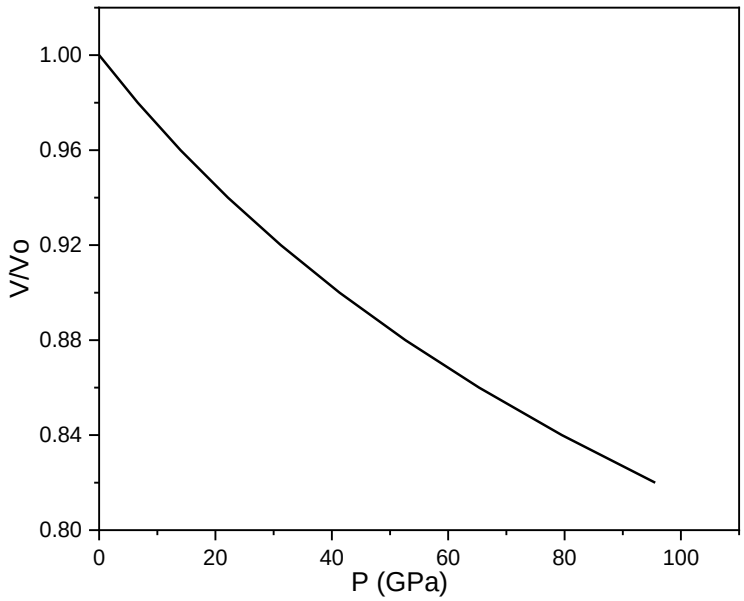

Figure 38: Pressure dependence of V/V_0 for n-TiN (60nm), using Eq. (3.88)

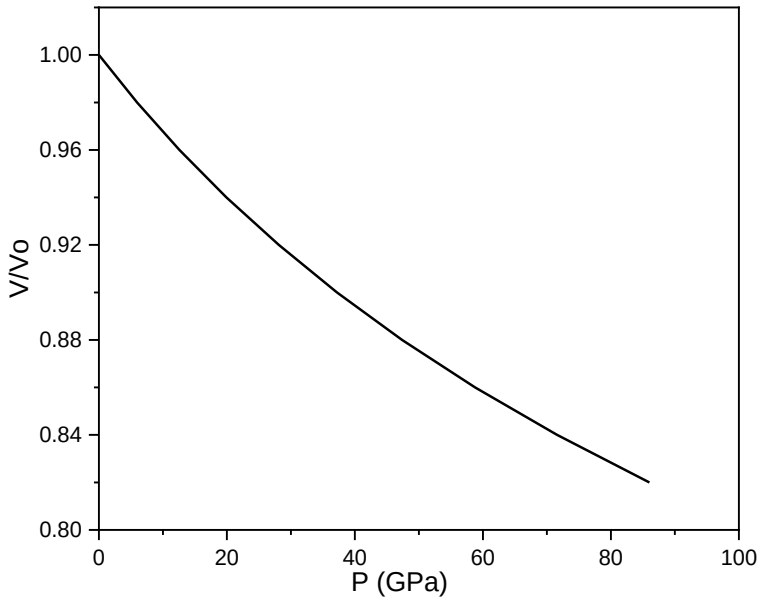

Figure 39: Pressure dependence of V/V_0 for n-TiN (80nm), using Eq. (3.88)

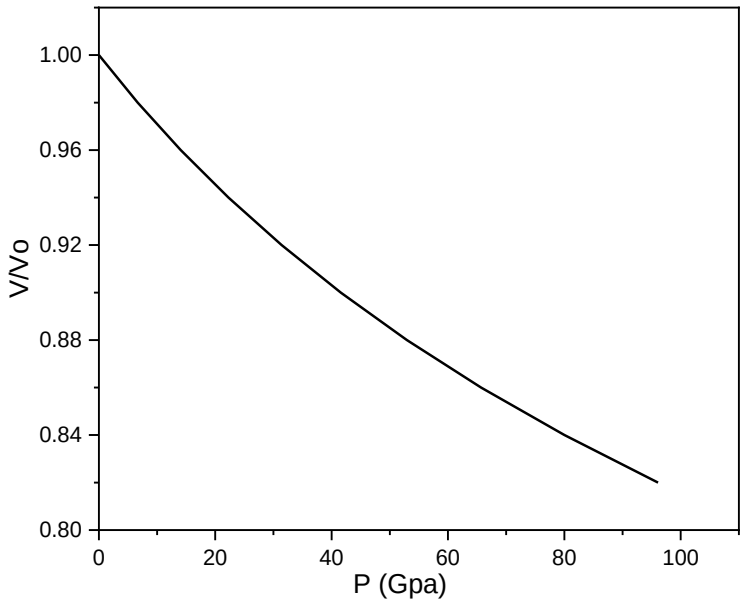

Figure 40: Pressure dependence of V/V_0 for n-TiN (100nm), using Eq. (3.88)

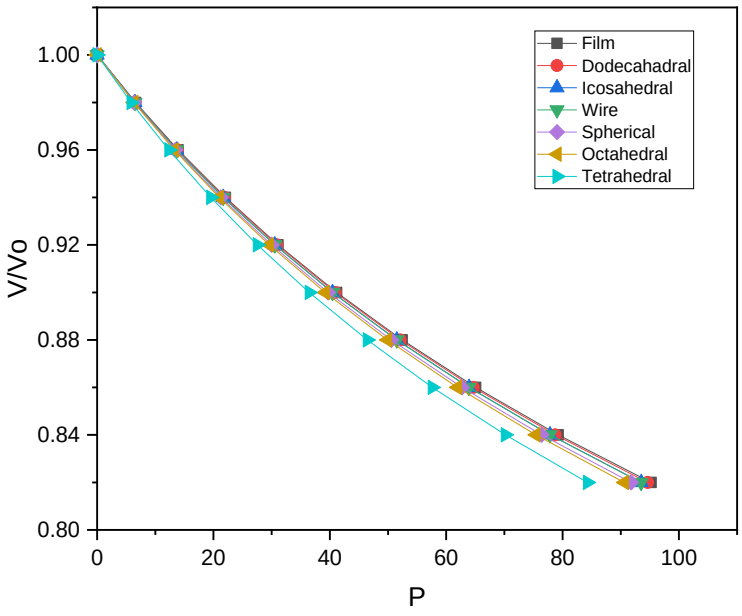

Figure 41: Pressure dependence of V/V_0 for different shapes of n-TiN (80nm), using Eqs. (3.89-3.95)

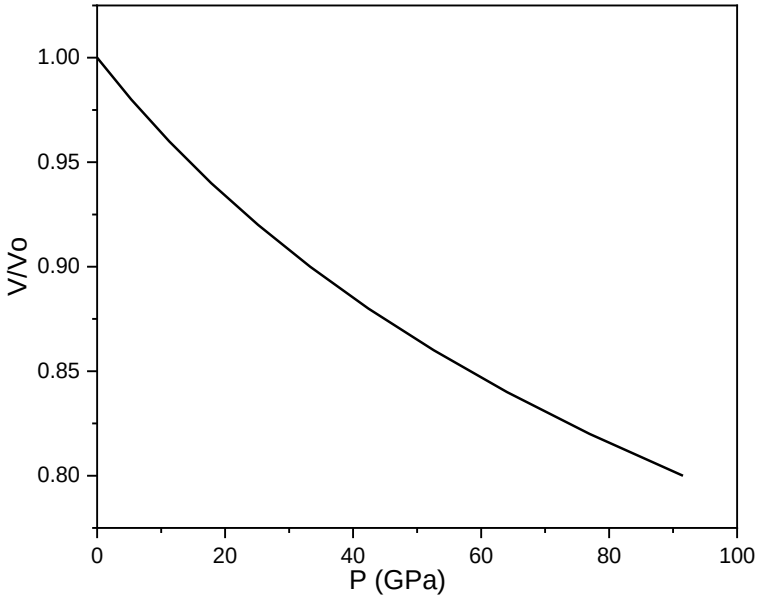

Figure 42: Pressure dependence of V/V_0 for α-Ga_2O_3 (14nm), using Eq. (3.88)

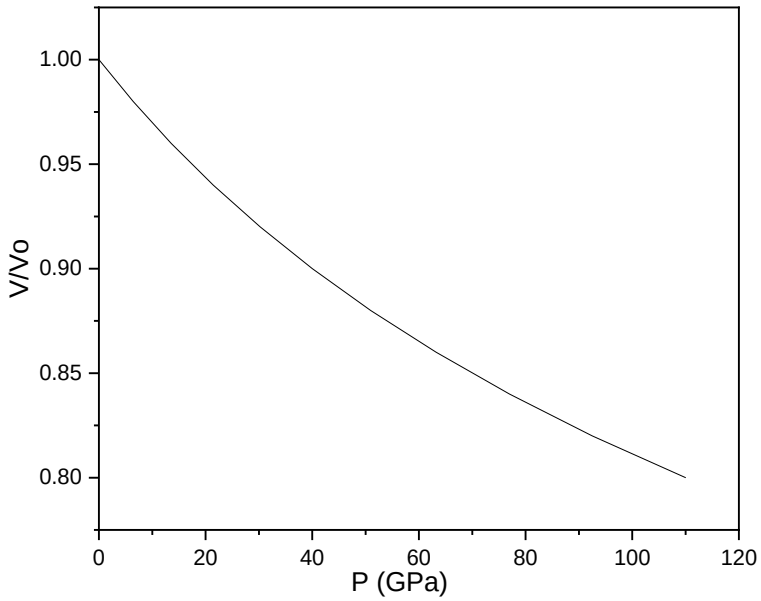

Figure 43: Pressure dependence of V/V_0 for α-Ga_2O_3 (40nm), using Eq. (3.88)

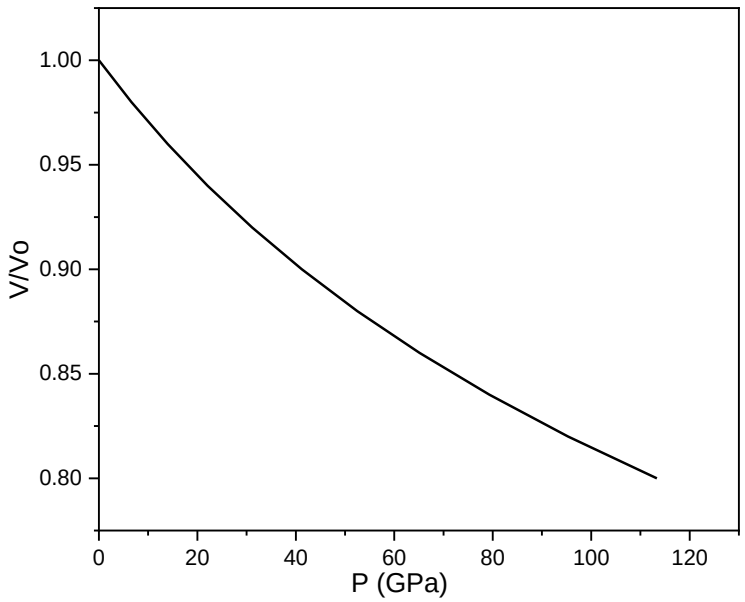

Figure 44: Pressure dependence of V/V_0 for α-Ga_2O_3 (60nm), using Eq. (3.88)

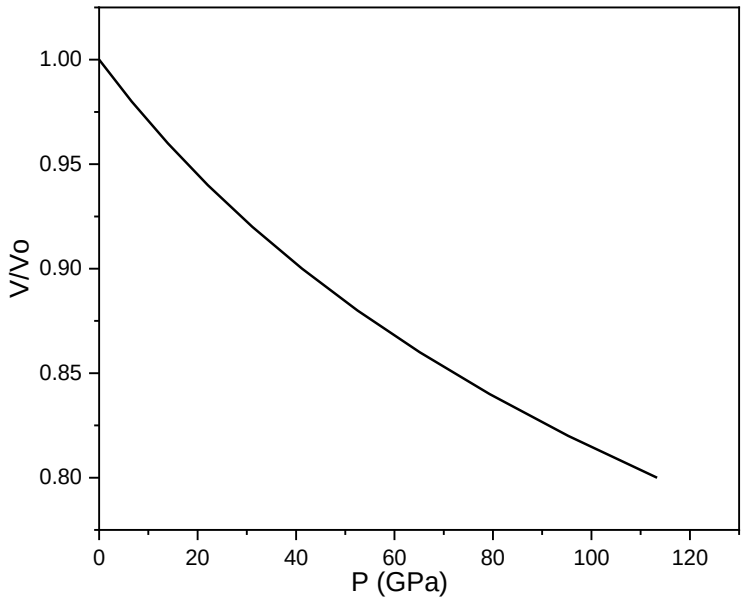

Figure 45: Pressure dependence of V/V_0 for α-Ga_2O_3 (80nm), using Eq. (3.88)

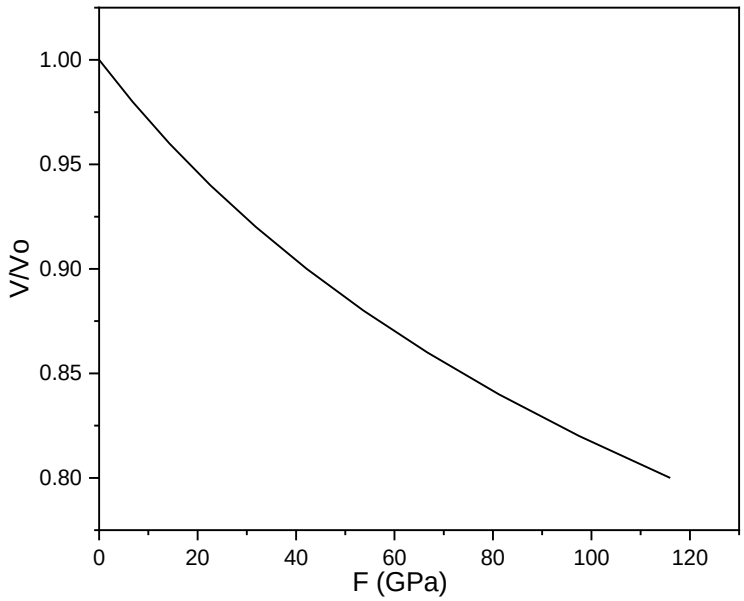

Figure 46: Pressure dependence of V/V_0 for α-Ga_2O_3 (100nm), using Eq. (3.88)

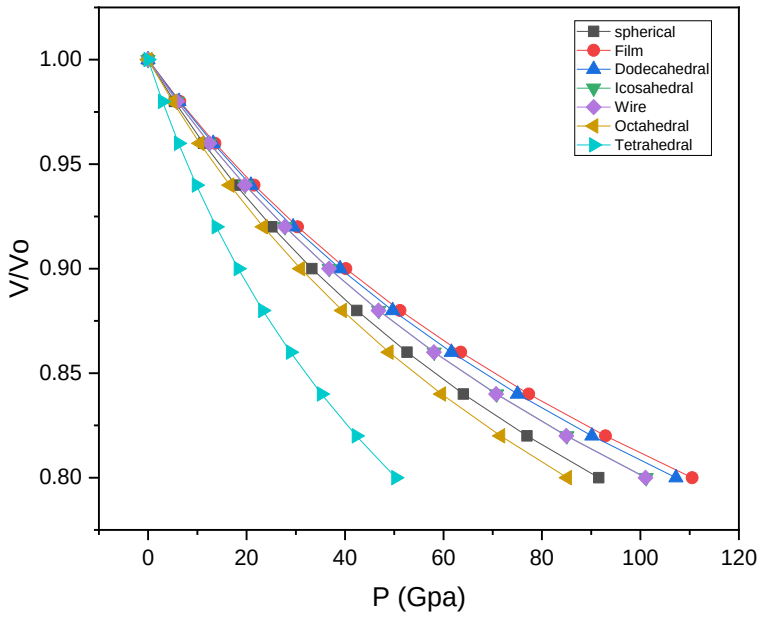

Figure 47: Pressure dependence of V/V_0 for different shapes of α-Ga_2O_3 (100nm), using Eqs. (3.89-3.95)

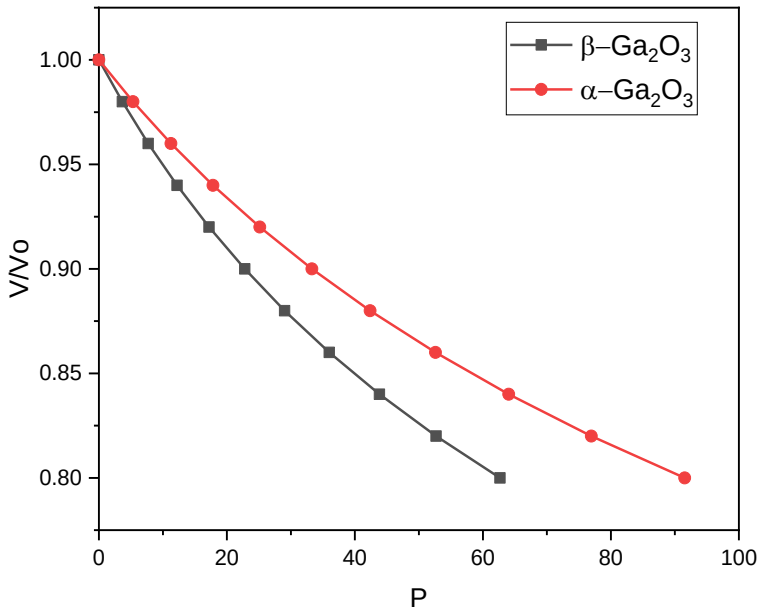

Figure 48: Pressure dependence of V/V_0 for α-Ga_2O_3 (14nm) and β-Ga_2O_3 (14nm). Using Eq. (3.88)

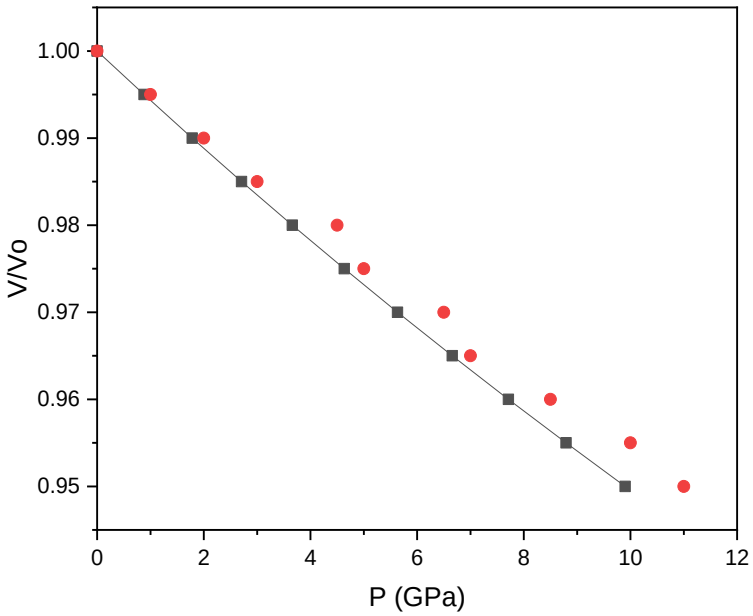

Figure 49: Pressure dependence of V/V_0 for β-Ga_2O_3 (14nm) using Eq. (3.88), • demonstrate the experimental data **(Lin *et al.*, 2009).**

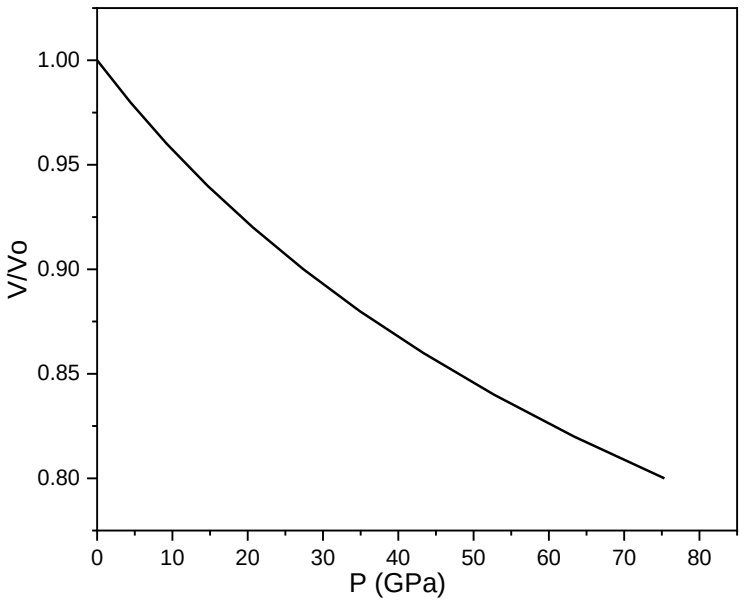

Figure 50: Pressure dependence of V/V_0 for β-Ga_2O_3 (40nm), using Eq. (3.88)

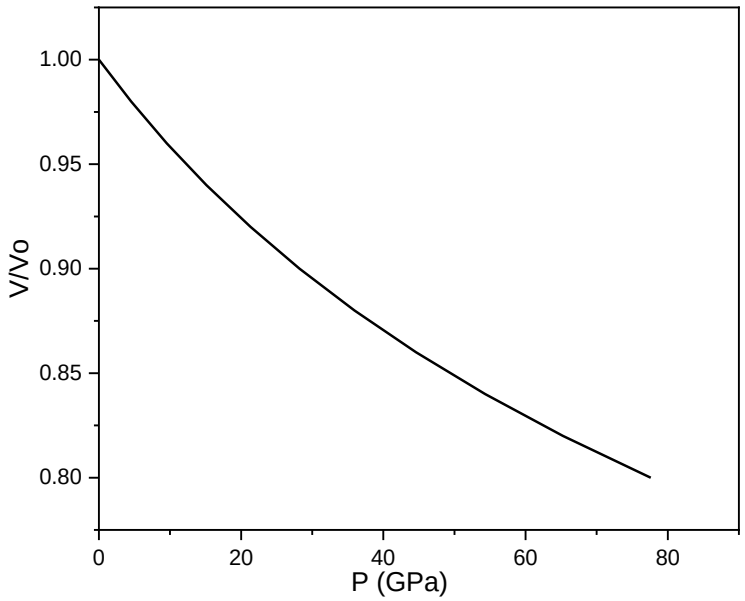

Figure 51: Pressure dependence of V/V_0 for β-Ga_2O_3 (60nm), using Eq. (3.88)

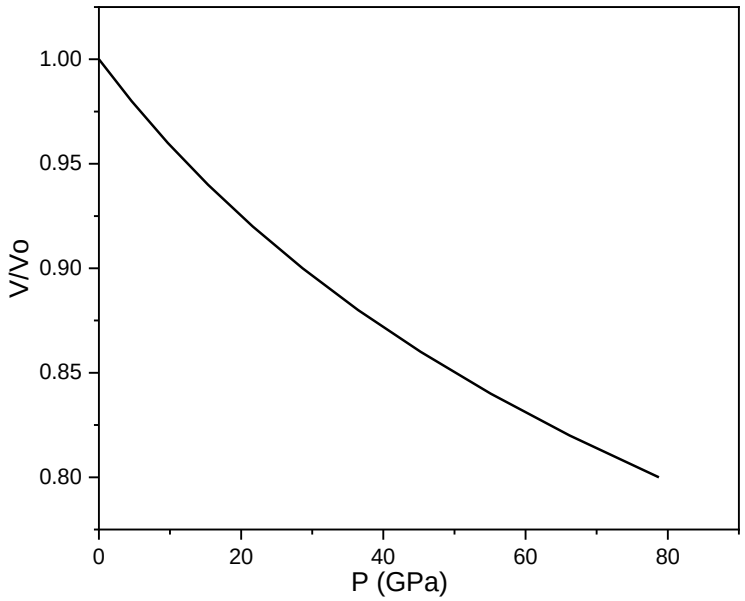

Figure 52: Pressure dependence of V/V_0 for β-Ga_2O_3 (80nm), using Eq. (3.88)

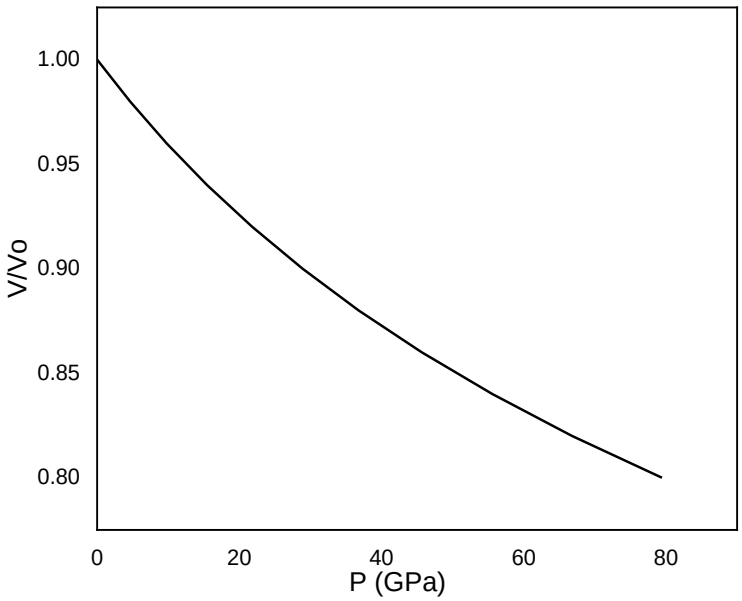

Figure 53: Pressure dependence of V/V_0 for β-Ga_2O_3 (100nm), using Eq. (3.88)

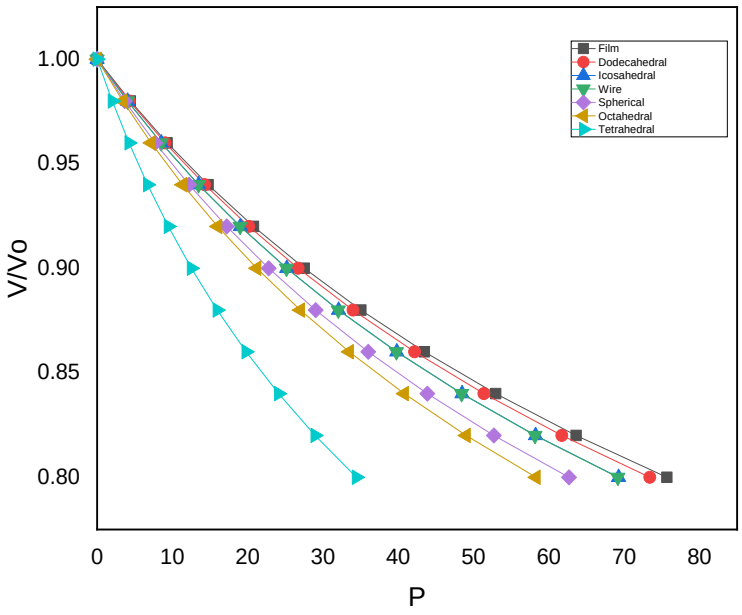

Figure 54: Pressure dependence of V/V_0 for different shapes of β-Ga_2O_3 (14nm), using Eqs. (3.89-3.95)

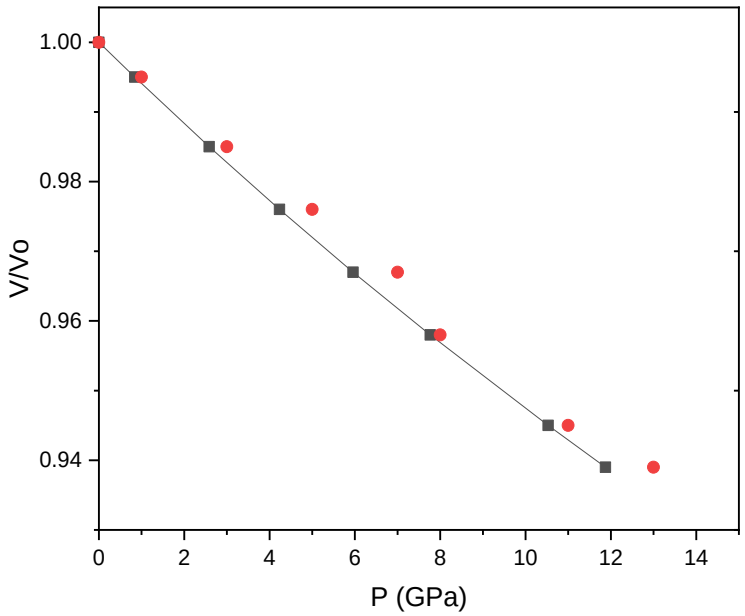

Figure 55: Pressure dependence of V/V_0 for Ho_2O_3 (14nm) using Eq. (3.88), • demonstrate the experimental data **(Yan *et al.*, 2014).**

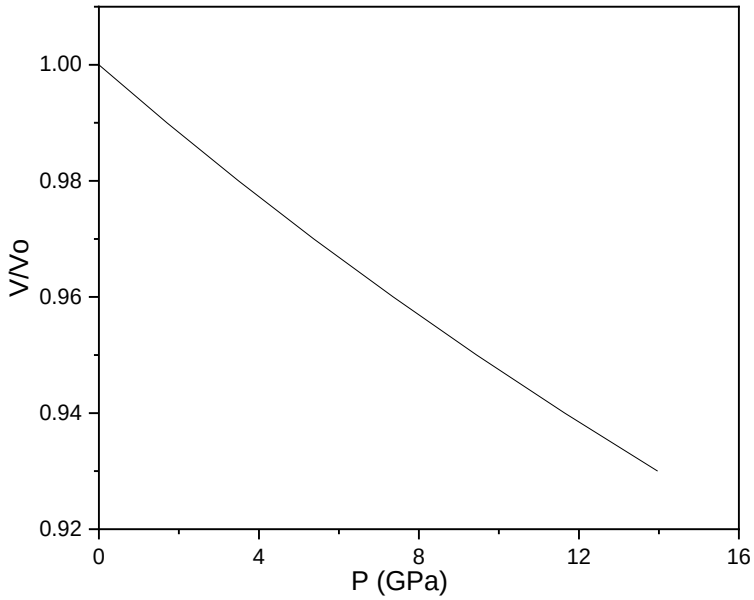

Figure 56: Pressure dependence of V/V_0 for Ho_2O_3 (14nm), using Eq. (3.88)

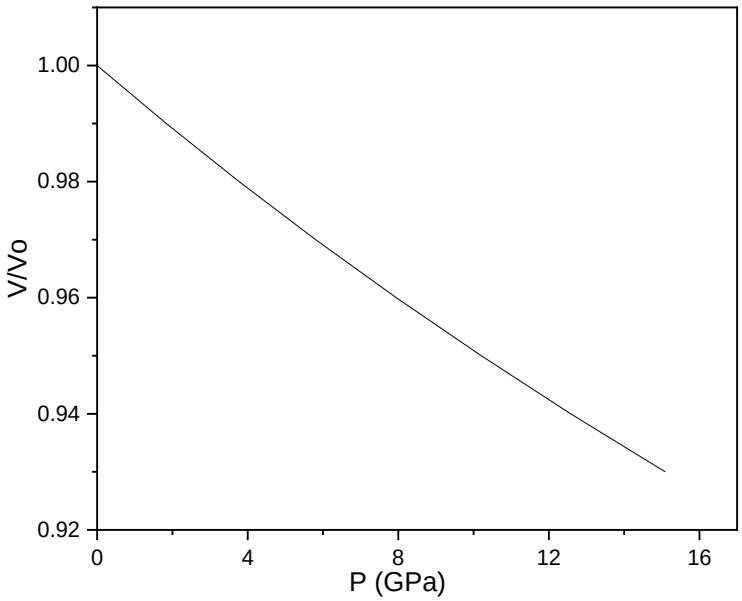

Figure 57: Pressure dependence of V/V_0 for Ho_2O_3 (40nm) using Eq. (3.88)

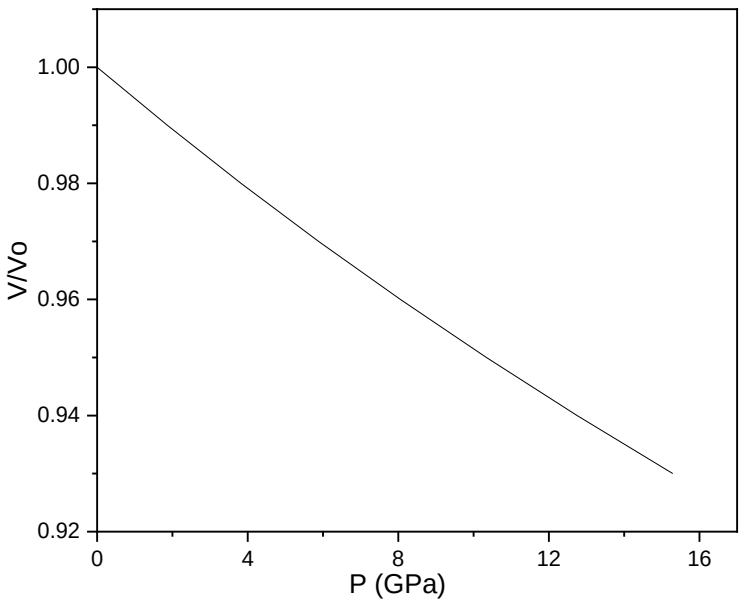

Figure 58: Pressure dependence of V/V_0 for Ho_2O_3 (60nm) using Eq. (3.88)

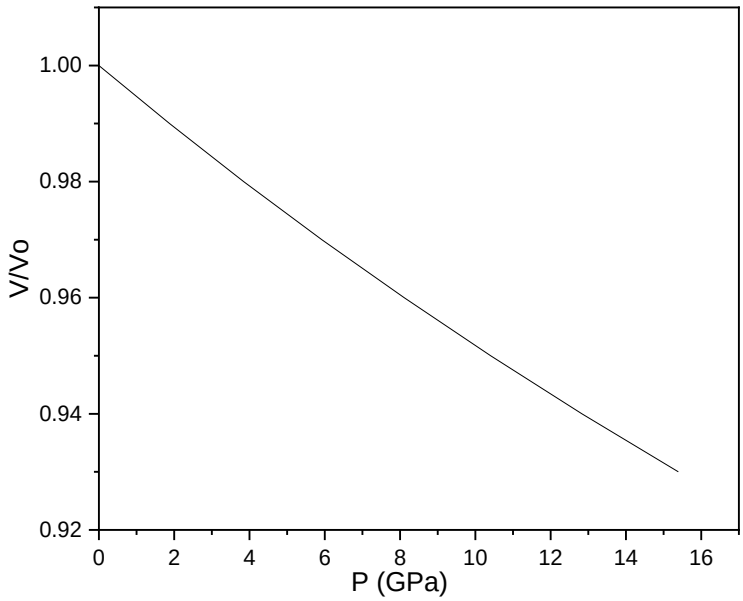

Figure 59: Pressure dependence of V/V_0 for Ho_2O_3 (80nm) using Eq. (3.88)

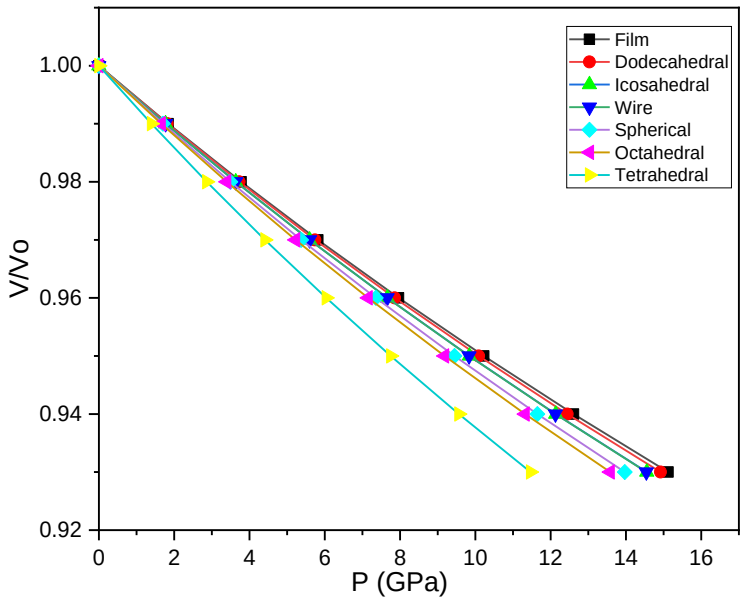

Figure 60: Pressure dependence of V/V_0 for Ho_2O_3 (40nm) for different shapes, using Eqs. (3.89-3.95)

Summary and Conclusions

Chapter 5 SUMMARY AND CONCLUSION

Nanomaterials are getting much attention because of their applications as well as their fundamental research interest increase due to their unique properties and structural stability which is quite different from the bulk counterpart. Moving from bulk to nanomaterials may leads several changes in physical and chemical properties. The properties like electronic, magnetic, optical, photonic etc and the variety of application, such as sensors, LEDs, drug delivery, medical diagnostics, catalyst and gene therapy attracts the researchers interest on it. These properties for bulk amounts are not depends on size as the decreases reduced one of the dimension to a certain limit normally under 100nm this becomes the size dependent one. In the present thesis we discussed the recently developed theoretical formulation and using it to understand the behaviour of nanomaterials under the effect of pressure, size and shape. We have used the concept of the size dependence of bulk modulus and discussed the various theories for the equation of state (EOS). We discussed Murnaghan equation of state briefly with the help of three theories, Eq. (3.88) is our final equation in which we included the effect of size as well as shape. A careful review of literature of EOS suggested that the MEOS has been widely used during the experimental work. In the present work we study the compression behaviour of nanomaterials for the different sizes and shapes viz. Film, dodecahedral, icosahedral, wire, spherical, octahedral and tetrahedral. The model predictions were compared with an experimental data to verify the suitability of the model predictions. We consider those material whose experimental data was available and materials are MgO (20nm), ZnO_2 (3.1nm), WC (25nm), n-ReB_2 (40nm), n-$ReWB_2$ (30nm), TiN (18nm), TiN (34nm), TiN (80nm), α-Ga_2O_3 (14nm), β- Ga_2O_3 (14nm), Ho_2O_3 (14nm). A good agreement between theory and experimental data is the validation of the model.

In the present thesis, we analyzed the compression behaviour of nanomaterials using Eq. (3.88) for different size and shape. We improved the model or Eq. (3.88) for the effect of shape using the values of N/n from the table 4.1. We observed a change by changing the shape from fil to tetrahedral at high pressure region, and shape effect is less at low pressure range. The shape effect is investigated in the absence of

experimental data which maybe helpful for the researchers engaged in experimental works of these materials. The shift in a isotherm curve was observed with increase in size. It was found that the compression is small for the smaller size and increseaes with increases in size. It means at low pressure range the effect of size is very small but it increases with increasing the pressure. Thus, we may concluded that the shift in a isotherm curve is depends on size. Further, we extended our model to investigate the effect of shape. We studied the compression behaviour of nanoparticles for different shapes and observed that there is an shift in isotherm curve and found larger for the film indicated that they are most compressible and smaller for the tetrahedral indicated that they are least compressible. This is due to the different surface to volume ratio of nanoparticles for different shapes. The effect of shape is shown higher for high pressure and decreases with decreasing pressure.

We conclude that the model developed in the present thesis is capable of predicting different properties of nanomaterials under varying condition of pressure, size and shape. We may conclude that the results obtained in the present show good agreement with experimental data which proofs the validation of model and some results that are reported in the absence of experimental data may be useful for the future studies.

Literature Cited

LITERATURE CITED

Anderson, O. L. (1994). Equations of State of Solids for Geophysics and Ceramic Science. New York, Oxford University Press. pp. 6-51.

Bhatt, A. and Kumar, M. (2012). Size-Dependent Equation of State for Nanomaterials. *International Journal of Nanoscience*, *11*(01), 1250010.

Bhatt, J. C. (2015). Effect of size on the elastic and thermodynamic properties of nanomaterials. *Indian Journal of Pure & Applied Physics (IJPAP)*, *52*(9), 604-608.

Bhatt, J. C., Kholiya, K. and Kumar, R. (2013). High Pressure Equation of State for Nanomaterials. *ISRN Nanotech*. 404920.

Bhatt, S. and Kumar, M. (2017). Equation of state and lattice parameter of SnO2 nanomaterial. *Materials Today: Proceedings*, *4*(9), 9547-9551.

Chen, B., Penwell, D., Benedetti, L. R., Jeanloz, R. and Kruger, M. B. (2002). Particle-size effect on the compressibility of nanocrystalline alumina. *Physical Review B*, *66*(14), 144101.

Chen, H. H., Bi, Y., Mao, H. K., Xu, J. A., Liu, L., Jing, Q. M., ... & Wang, Q. M. (2013). High-pressure strength of nanocrystalline tantalum carbide (TaC) studied at a non-hydrostatic compression. *International Journal of Refractory Metals and Hard Materials*, *41*, 627-630.

Chen, W., Lu, Y. H., Wang, M., Kroner, L., Paul, H., Fecht, H. J., ... & Kaiser, U. (2009). Synthesis, thermal stability and properties of ZnO2 nanoparticles. *The Journal of Physical Chemistry C*, *113*(4), 1320-1324.

Chhabra, H. and Kumar, M. (2020). Development of size and shape dependent model for magnetic properties from bulk to nanoscale. *Indian Journal of Physics*, 1-8.

Couvy, H., Chen, J. and Drozd, V. (2010). Compressibility of nanocrystalline forsterite. *Physics and Chemistry of Minerals*, *37*(6), 343-351.

Font, F., Myers, T. G. and Mitchell, S. L. (2015). A mathematical model for nanoparticle melting with density change. *Microfluidics and Nanofluidics*, *18*(2), 233-243.

Goyal, M. and Gupta, B. R. K. (2018). Shape and size dependent thermophysical properties of nanocrystals. *Chinese journal of physics*, *56*(1), 282-291. Hama, J. and Suito, K. (1999). Thermoelastic properties of periclase and magnesiowüstite under high pressure and high temperature. *Physics of the Earth and Planetary Interiors*, *114*(3-4), 165-179.

He, Y., Liu, J. F., Chen, W., Wang, Y., Wang, H., Zeng, Y. W., ... & Hahn, H. (2005). High-pressure behavior of SnO_2 nanocrystals. *Physical Review B*, *72*(21), 212102.

Jiang, Q., Aya, N. and Shi, F. G. (1997). Nanotube size-dependent melting of single crystals in carbon nanotubes. *Applied Physics A: Materials Science & Processing*, *64*(6).

Jiang, Q., Li, J. C. and Chi, B. Q. (2002). Size-dependent cohesive energy of nanocrystals. *Chemical Physics Letters*, *366*(5-6), 551-554.

Jiang, Q., Shi, H. X. and Zhao, M. (1999). Melting Thermodynamics of Organic Nanocrystals. *The J. Che. Phy.* **111**(5): 2176–2180.

Kholiya, K. and Pandey, K. (2019). High pressure compression behaviour of bulk and nanocrystalline SnO_2. *Journal of Taibah University for Science*, *13*(1), 592-596.

Kumar, M. (1995). High pressure equation of state for solids. *Physica B: Condensed Matter*, *212*(4), 391-394.

Kumar, M. and Kumar, M. (2008). Empirical high pressure equation of state for nano materials. *Indian Journal of Pure & Applied Physics*, *46*(6), 378-381.

Kumar, R. and Kumar, M. (2010). Size dependence of thermoelastic properties of nanomaterials. *International Journal of Nanoscience*, *9*(05), 537-542.

Kumar, R., Sharma, G. and Kumar, M. (2013). Size and temperature effect on thermal expansion coefficient and lattice parameter of nanomaterials. *Modern Physics Letters B*, *27*(25), 135-180.

Lei, J., Hu, S., Turner, C. L., Zeng, K., Yeung, M. T., Yan, J., ... & Tolbert, S. H. (2019). Synthesis and High-Pressure Mechanical Properties of Superhard Rhenium/Tungsten Diboride Nanocrystals. *ACS nano*, *13*(9), 10036-10048.

Li, S., Qi, W., Peng, H. and Wu, J. (2015). A comparative study on melting of core–shell and Janus Cu–Ag bimetallic nanoparticles. *Computational Materials Science*, *99*, 125-132.

Li, X. (2014). Modeling the size-and shape-dependent cohesive energy of nanomaterials and its applications in heterogeneous systems. *Nanotechnology*, *25*(18), 185702.

Li, Y. J., Qi, W. H., Huang, B. Y., Wang, M. P. and Xiong, S. Y. (2010a). Modeling the melting temperature of metallic nanowires. *Modern Physics Letters B*, *24*(22), 2345-2356.

Li, Y. J., Qi, W. H., Huang, B. Y., Wang, M. P. and Xiong, S. Y. (2010b). Modeling the thermodynamic properties of bimetallic nanosolids. *Journal of Physics and Chemistry of Solids*, *71*(5), 810-817.

Liang, H., Upmanyu, M. and Huang, H. (2005). Size-dependent elasticity of nanowires: nonlinear effects. *Physical Review B*, *71*(24), 241403.

Liang, L. H. and Li, B. (2006). Size-dependent thermal conductivity of nanoscale semiconducting systems. *Physical Review B*, *73*(15), 153303.

Liang, L., Ma, H. and Wei, Y. (2011). Size-Dependent Elastic Modulus and Vibration Frequency of Nano crystals. *Journal of Nanomaterials*, 6.

Lin, Z., Wang, L., Zhang, J., Mao, H. K. and Zhao, Y. (2009). Nanocrystalline tungsten carbide: As incompressible as diamond. *Applied Physics Letters*, *95*(21), 211906.

Lu, H. M. and Jiang, Q. (2004). Size-dependent surface energies of nanocrystals. *The Journal of Physical Chemistry B*, *108*(18), 5617-5619.

Luo, W., Hu, W. and Xiao, S. (2008). Size effect on the thermodynamic properties of silver nanoparticles. *The Journal of Physical Chemistry C*, *112*(7), 2359-2369.

Marquardt, H., Speziale, S., Marquardt, K., Reichmann, H. J., Konôpková, Z., Morgenroth, W. and Liermann, H. P. (2011). The effect of crystallite size and stress condition on the equation of state of nanocrystalline MgO. *Journal of Applied Physics*, *110*(11), 113512.

Murnaghan, F.D., 1937. A theory of Elasticity. *Phy. Rev.* 51, 593.

Nanda, K. K., Sahu, S. N. and Behera, S. N. (2002). Liquid-drop model for the size-dependent melting of low-dimensional systems. *Physical Review A*, *66*(1), 013208.

Olsen, J. S., Gerward, L. and Jiang, J. Z. (2002). High-pressure behavior of nano titanium dioxide. *High Pressure Research*, *22*(2), 385-389.

Patel, G. R., Thakar, N. A. and Pandya, T. C. (2016). Size and shape dependent melting temperature and thermal expansivity of metallic and semiconductor nanoparticles. In *AIP Conference Proceedings* (Vol. 1731, No. 1, p. 050042). AIP Publishing LLC.

Plymate, T. G. and Stout, J. H. (1989). A five-parameter temperature-corrected Murnaghan equation for P-V-T surfaces. *Journal of Geophysical Research: Solid Earth*, *94*(B7), 9477-9483.

Qi, W. (2016). Nanoscopic thermodynamics. *Accounts of Chemical Research*, *49*(9), 1587-1595.

Qi, W. H. (2006). Generalized Surface-Area-Difference model for cohesive energy of nanoparticles with different compositions. *Journal of materials science*, *41*(17), 5679-5681.

Qi, W. H. 2005. Size Effect on Melting Temperature of Nanosolids. *Physica B.* **368**: 46–50.

Qi, W. H., Wang, M. P. and Su, Y. C. 2002. Effect on the Lattice Parameters of Nanoparticles. *J Mat. Sci. Let*. **21**: 877-878.

Qi, W. H. and Wang, M. P. 2004. Size and Shape Dependent Melting Temperature of Metallic Nanoparticles. *Mat. Che. & Phy*. **88**(2-3): 280–284.

Rekhi, S., Saxena, S. K., Atlas, Z. D. and Hu, J. (2000). Effect of particle size on the compressibility of MgO. *Solid state communications*, *117*(1), 33-36.

Safaei, A. (2011). Cohesive energy and physical properties of nanocrystals. *Philosophical Magazine*, *91*(10), 1509-1539.

Shanker, J., Sharma, M. P. and Kushwah, S. S. (1999). Analysis of melting of ionic solids based on the thermal equation of state. *Journal of Physics and Chemistry of Solids*, *60*(5), 603-606.

Sharma, G. and Kumar, M. (2014). Size and shape dependent thermoelastic properties of nanomaterials. *High Temperatures--High Pressures*, *43*(4).

Sharma, G. and Kumar, M. (2015). Modelling for hardening and softening of nanomaterials due to size reduction. *High Temperatures--High Pressures*, *44*(4).

Singh, M. and Singh, M. (2015). Impact of size and temperature on thermal expansion of nanomaterials. *Prama*, *84*(4), 609-619.

Singh, M., Lara, S. O. and Tlali, S. (2017). Effects of size and shape on the specific heat, melting entropy and enthalpy of nanomaterials. *Journal of Taibah University for Science*, *11*(6), 922-929

Singh, M., Tlali, S. and Narayan, H. (2012). Pressure Dependent Volume Change in Some Nanomaterials Using an Equation of State. *Nanoscience and Nanotechnology*, *2*(6), 201-207.

Vinet, P., Smith, J.R., Ferrante, J. and Rose, J.H., 1987. Temperature effects on the universal equation of state of solids. *Physical Review B*, 35, 1945.

Wang, H., He, Y., Chen, W., Zeng, Y. W., Stahl, K., Kikegawa, T. and Jiang, J. Z. (2010). High-pressure behavior of β-Ga_2O_3 nanocrystals. *Journal of Applied Physics*, *107*(3), 033520.

Wang, Y., Zhang, J., Wei, Q. and Zhao, Y. (2013). Grain size effects on the compressibility and yield strength of copper. *Journal of Physics and Chemistry of Solids*, *74*(1), 75-79.

Xiong, S., Qi, W., Cheng, Y., Huang, B., Wang, M. and Li, Y. (2011b). Modeling size effects on the surface free energy of metallic nanoparticles and nanocavities. *Physical Chemistry Chemical Physics*, *13*(22), 10648-10651.

Xiong, S., Qi, W., Huang, B. and Wang, M. (2011a). Size-, Shape-and Composition-Dependent Alloying Ability of Bimetallic Nanoparticles. *Chem. Phys. Chem*, *12*(7), 1317-1324.

Yan, X., Ren, X., He, D., Chen, B. and Yang, W. (2014). Mechanical behaviors and phase transition of Ho_2O_3 nanocrystals under high pressure. *Journal of Applied Physics*, *116*(3), 033507.

Zhang, J. (2000). Effect of pressure on the thermal expansion of MgO up to 8.2 GPa. *Physics and Chemistry of Minerals*, *27*(3), 145-148.

Zhang, X., Li, W., Wu, D., Deng, Y., Shao, J., Chen, L. and Fang, D. (2018). Size and shape dependent melting temperature of metallic nanomaterials. *Journal of Physics: Condensed Matter*, *31*(7), 075701.

Zou, C. D., Gao, Y. L., Bin, Y. A. N. G. and Zhai, Q. J. (2010). Size-dependent melting properties of Sn nanoparticles by chemical reduction synthesis. *Transactions of Nonferrous Metals Society of China*, *20*(2), 248-253.

CURRICULUM VITAE

Name : Laxmi Mehra

Phone Number : 8650230550

Mailing Address:
Vill- Beru mahar, Sainrathi
PO- Sainrathi
Pithoragarh, uttarakhand
Email : laxmi598m@gmail.com

Permanent Address:
Vill- Beru mahar, Sainrathi
PO- Sainrathi
Pithoragarh, uttarakhand

Career Objective: To research in the field of Physics

Educational Qualification:

S. No.	Examination Passed	Institution	Year	Percentage/ CGPA
1.	**M.Sc (Physics**	GB Pant University of Agriculture and Technology, Pantnagar, UK, 263145	2021	**7.3/10**
2.	**B.Sc.**	College of Agriculture Pune, Maharashtra, 411005	2018	**68.59**
3.	**Intermediate (CBSE)**	New Beersheba senior secondary school, Pithoragarh, Uttarakhand	2015	**72.6**
4.	**High School (CBSE)**	St. Queen Mary's public school, Agra, U.P	2013	**8.8/10**

- **Specialization :** Major: Physics Minor: Nil
- **Publications:** nil
- **Conferences/Seminars/Workshops/Trainings Attended:** Nil
- **List of papers presented in conference/seminar during degree programme:** Nil
- **Software skills:** Origin 8.**5**
- **Professional skills:** Nanomaterials
- **Professional Affiliations:** Nil
- **Awards/Honours/Achievements:** Nil

Place : Pantnagar

Date : August, 2021

(Laxmi Mehra)

ABSTRACT

Name : Laxmi Mehra **Id. No.** : 53943

Sem. & Year of admission : Ist, 2018-19 **Degree** : M.Sc. (Physics)

Major : Physics **Department** : Physics

Thesis Title : Study for the effect of pressure, size and shape of nanomaterials.

No. of pages : 71 **Advisor** : Dr. Munish Kumar

Nanomaterials at high pressure are one of the major areas of interest due to its immense potential of applications. Due to a small size nanomaterials shows novel properties. Nanoparticles are used in a variety of application, such as sensors, LEDs, drug delivery, medical diagnostics, catalyst and gene therapy. Their unique range of properties and enormous application led to the development of the nanotechnology. In the present thesis we used the Murnaghan EOS for various nanomaterials. We have computed the pressure dependence of V/V_0 for different sizes and shapes viz. Film, dodecahedral, icosahedral, wire, spherical, octahedral and tetrahedral. The materials which we included in the present study are viz. MgO (20nm), MgO (11nm), ZnO_2 (3.1nm), WC (25nm), n-ReB_2 (40nm), n-$Re_{0.52}W_{0.48}B_2$ (30nm), TiN (18nm), TiN (34nm), TiN (80nm), α-Ga_2O_3 (14nm), β- Ga_2O_3 (14nm), Ho_2O_3 (14nm) because of the experimental data are available on these materials so the comparison is also possible. We studied the nanomaterials for the different sizes and shapes in room temperature. A shift in isotherm is observed with the increase in size. We studied the compression behaviour of nanoparticles for different shapes and observed that there is a shift in isotherm curve and found larger for the film indicated that they are most compressible and smaller for the tetrahedral indicated that they are least compressible. This is due to the different surface to volume ratio of nanoparticles for different shapes. Our results are found to be in good agreement with the experimental data. Hence it proves the validity of the theory of EOS used in the present thesis.

(Munish Kumar)
Advisor

(Laxmi Mehra)
Authoress

सारांश

नाम	:	लक्ष्मी मेहरा	**परिचयांक**	:	53943
षट्मास एवं प्रवेष वर्ष	:	प्रथम, 2018–19	**उपाधि**	:	स्नातकोत्तर
प्रमुख विषय	:	भौतिकी	**विभाग**	:	भौतिकी
शोध का शीर्षक	:	''नैनो मटेरियल्स के दबाव, आकार एवं आकृति के लिए अध्ययन''			
पृष्ठ संख्या	:	71	**सलाहकार**	:	डॉ0 मुनीश कुमार

उच्च दाब पर नैनो पदार्थ अपनी अपार क्षमता के अनुप्रयोगों के कारण मुख्य रूचिकर क्षेत्रों में से एक है। सूक्ष्म आकार के कारण नैनो मटेरियल्स अलग गुणों को दर्शाता है, जिसके कारण उनमें व्यापक रूचि पैदा हुई है। नैनोकणों का उपयोग विभिन्न प्रकार के अनुप्रयोगों में किया जाता है, जैसे सेंसर, एलईडी, दवा वितरण, चिकित्सा निदान, उत्प्रेरक और जीन थेरेपी। इनके अद्वितीय गुणों और विशाल अनुप्रयोग ने नैनो तकनीक के विकास का नेतृत्व किया। वर्तमान शोध में विभिन्न नैनोमटेरियल्स के लिए मुर्नाघन समीकरण का उपयोग किया। हमने V/V_0 पर दाब का प्रभाव अलग–अलग आकार और आकृति जैसे फिल्म, डोडेकाहेड्रल, इकोसाहेड्रल, वायर, गोलाकार, ऑकटाहेड्रल और टेट्राहेड्रल पर परिकलित किया। वे पदार्थ जो वर्तमान अध्ययन में शामिल किये गये क्रमशः MgO (20nm), MgO (11nm), ZnO_2 (3.1nm), WC (25nm), n-ReB_2 (40nm), n-$Re_{0.52}W_{0.48}B_2$ (30nm), TiN (18nm), TiN (34nm), TiN (80nm), α-Ga_2O_3 (14nm), β- Ga_2O_3 (14nm), Ho_2O_3 (14nm) है। सामताप रेखा में आकार बढ़ने के साथ एक परिवर्तन पाया गया। ऐसा ही व्यवहार नैनोमेटेरिल्स की विभिन्न आकृतियों में पाया गया। नैनो पदार्थो की विभिन्न आकृतियों के लिए सामताप रेखा में परिवर्तन का क्रम नैनो फिल्म में अधिकतम देखा एवं टेट्राहेड्रल में न्यूनतम पाया गया। प्रयोगात्मक आँकड़ों के साथ अच्छी सहमति में पाये गये जो कि वर्तमान शोध में प्रयुक्त अवस्था के समीकरण की वैधता को साबित करते है।

(मुनीश कुमार)
सलाहकार

(लक्ष्मी मेहरा)
लेखिका